

Use Authorization

In presenting this dissertation in partial fulfillment of the requirements for an advanced degree at Idaho State University, I agree that the Library shall make it freely available for inspection. I further state that permission to download and/or print my dissertation for scholarly purposes may be granted by the Dean of the Graduate School, Dean of my academic division, or by the University Librarian. It is understood that any copying or publication of this dissertation for financial gain shall not be allowed without my written permission.

Signature: _____

Date: _____

Title

Real Time-Spatial SEMG Classification for Motion Control Using Fuzzy Inference System

By

Shaikh Faysal Mahamud

A thesis submitted in partial fulfillment of the requirements for the degree of

Master of Science

in

the Department of Mechanical Engineering

Idaho State University

December 2018

Committee Approval

To the Graduate Faculty:

The members of the committee appointed to examine the thesis of Shaikh Faysal Mahamud find it satisfactory and recommend that it be accepted:

Dr. Marco P. Schoen,
Major Advisor

Dr. Alba Perez Gracia,
Committee Member

Dr. Steve C. Chiu,
Graduate Faculty Representative

Acknowledgment

“Engineering” It is not a simple word to give a person some identical name for fame but it’s a process. The process which starts with knowledge. What makes a person an Engineer? No, it’s not some official degree. It’s the thrust for knowing something new every day.

From my primary school, I was passionate about knowledge and science. The unlimited sources of mysterious science around us surprise me all the time. “What”, “How” and “Why” those three words are the playfellows from my childhood. That’s why I took science as my best friend. My true friendship with science reflects on my works. To fulfill my inner thrust for science I had started my thesis work. My wants to know the science never comes to an end. I also believe that this passion of knowledge helped me to complete my degree.

I have a lot of people’s blessings to accomplish this success. First of all, I would love to thank my best friend- my Wife. Without her support, I couldn’t be able to do this. She always comforts me at my hard time.

I can clearly remember my 1st semester at Idaho State University. As I just started my school after almost 5 years, I was so lost. At that hardest time of my life I was saved by my Department. I have no words to express my gratitude to my Department.

Professor Dr. Marco Schoen- He is not only my thesis advisor but also he is the advisor of all problem solving related to work-study. He guided me through each and every problem analysis of study. After my disastrous 1st semester I was able to come back to good academic result only because of his wise academic advice. Instead of his busy schedule, he never hesitated to guide his students. It is an honor to work under his guidance.

Last but not the least, it could not be possible for me to complete my study without the help of Dr. Alba Perez Gracia and Dr. Steve C. Chiu. I have learnt true leadership and effective fast decision making at any difficult situation from my honorable department chair Dr. Alba Perez Gracia. She helped me a lot at 3D printing lab.

Finally, It will be incomplete if I don't mention a true friend's name- GolamGauseJaman. From him I have learnt the definition of true commitment to study. He taught me how not to give up.

I am happy to appreciate all the supports I get from everyone to accomplish this achievement.

Table of Contents

List of Figures	viii
List of Abbreviations	xi
Abstract	xii
Chapter 1: Introduction	1
1.1 Problem Statement	1
1.2 Literature Review	2
1.3 Proposed Thesis Plan	2
Chapter 2: Background Information	4
2.1 What are EMG Signals	4
2.2 How EMG Signals are Generated	5
2.3 Electrode Placement	7
2.4 Where EMG Used	7
2.5 Classification Method for Feature Extraction	7
2.5.1 Standard Deviation	8
2.5.2 Mean	8
2.5.3 Fast Fourier Transform	8
2.6 Fuzzy Inference System	8
Chapter 3: Experimental Setup	10
3.1 First Part: Instrumentation Amplifier	10
3.2 Second Part: Notch Filter	11

3.3 Third Part: Passband Filter	12
3.4 Shortcomings	16
3.5 Placement of Electrodes	19
Chapter 4: Methodology/ Proposed Design	22
4.1 Overview	22
4.2 Visualizing the Change of the Shape of the Pentagon	22
4.3 Developing a Fuzzy Inference System	28
4.3.1 Defining Inputs and Outputs	28
4.3.2 Fuzzy Rules and Fuzzy Reasoning	29
4.3.3 MF Defuzzification	31
Chapter 5: Discussion and Result	32
5.1 Spatial based Visualization of Shape Changing of a Pentagon	32
5.2 Development of a Fuzzy Inference System	33
5.3 Identification of Motions and Result	46
References	51
Appendix	53

List of Figures

Figure 2.1: The composition of muscle cells, muscle fascicles, muscle fiber, myofibril, myofilaments, sarcomere, thick and thin filaments [1]	5
Figure 2.2: Parts of Motor Unit [2]	6
Figure 3.1: Schematic of instrumentation amplifier [2]	10
Figure 3.2: Schematic diagram of notch filter [2]	11
Figure 3.3: Schematic diagram of high-pass filter [2]	12
Figure 3.4: Schematic diagram of low-pass filter [2]	13
Figure 3.5: Schematic diagram of voltage buffer amplifier [1]	14
Figure 3.6: A Printed Circuit Board model [2]	15
Figure 3.7: Schematic diagram of power supply [4]	15
Figure 3.8: Circuit connection of power supply [4]	16
Figure 3.9: Ten channels sEMG box	17
Figure 3.10: A new power supply of solderable board with connections	18
Figure 3.11: Final sEMG box with connections	19
Figure 3.12: Inner forearm muscle movement position	20
Figure 3.13: Outer forearm muscle movement position	20
Figure 3.14: sEMG signals for the inner forearm muscle movement	21
Figure 3.15: sEMG signals for the outer forearm muscle movement	21
Figure 4.1: Polar plot of five channels equally distributed with arbitrary radius value	23
Figure 4.2: Overlapping of two sets of arbitrary values	24

Figure 4.3: <i>Simulink</i> TM of five arbitrary sine waves to get visualization of continuous shape changing	25
Figure 4.4: Using analog inputs in <i>Simulink</i> TM block to get internal ten angles of the pentagon	26
Figure 4.5: Schematic diagram of a pentagon	27
Figure 4.6: Part of a pentagon	27
Figure 4.7: MF reasoning using fuzzy max-min decomposition (fuzzy rule no.1)	30
Figure 4.8: MF reasoning using fuzzy max-min decomposition (fuzzy rules no. 2,3, and 4)	31
Figure 5.1: Output graph of STD classification on area	34
Figure 5.2: Output graph of STD classification on area (closer view)	35
Figure 5.3: Output graph of FFT classification on area	36
Figure 5.4: Output graph of FFT classification on area (closer view)	37
Figure 5.5: Output graph of FFT classification on area (sample 48)	38
Figure 5.6: Output graph of FFT classification on area (sample 26)	39
Figure 5.7: Schematic diagram of a pentagon	40
Figure 5.8: Ten internal angles from θ_{12} to θ_{15} (columns first)	41
Figure 5.9: Mean of each frame (50 samples slide) for angles from θ_{12} to θ_{15} (columns first)	42
Figure 5.10: Mean of angle θ_{12} and θ_{21}	43
Figure 5.11: STD classification of five angles $\theta_{12}, \theta_{23}, \theta_{34}, \theta_{45}$ and θ_{51} (columns first)	44

Figure 5.12: STD classification of angles θ_{12} , θ_{23} and θ_{34} (columns first)	45
Figure 5.13: Motion identification using fuzzy logic controller	47
Figure 5.14: Motion identification using fuzzy logic controller (crisp value)	48
Figure 5.15: Phase difference between actual and targeted output	49

List of Abbreviations/Symbols

sEMG:	Surface Electromyography
Abs: $\hat{}$	Absolute Value
ANFIS:	Adaptive Neuro-Fuzzy Inference System
MU:	Motor Unit
MF:	Membership Function

Abstract

Real Time-Spatial sEMG Classification for Motion Control Using Fuzzy Inference System

Thesis Abstract--Idaho State University (2018)

Control of prosthetic devices using surface Electromyography (sEMG) signals is a common approach to provide enhanced functionality to upper body amputees. Current sEMG based upper body prosthetic devices are limited by the amount of information drawn from the acquired sEMG signals. The goal of this thesis work is to investigate the use of spatial features along with the temporal variations for the development of a fuzzy logic inference system. The spatial features are deduced by utilizing a circular sensor arrangement. In particular, the sEMG data along with its geometrical position is correlated with human forearm motion. This setup is used to construct fuzzy rules for a simple inference system to predict human hand motion from the sensed sEMG data and its position on the forearm. Five sEMG channels are equally distributed spatially over the perimeter of the forearm, and a polar coordinate system is used to for visualization of the changing sEMG signals. Both the area of the resulting sEMG pentagon and the corresponding inner angles of the pentagon are studied with using the Fast Fourier Transfer (FFT) and Standard Deviation (STD) classification method. The results of the frequency analysis of the sEMG-area property indicates some promise whereas angle based representation of the sEMG data shows to be a good source fuzzy logic inference rule development. The STD of internal angles give distinct relations, which are used to construct a fuzzy logic controller that is capable of discerning with some reliability two forearm movements.

Key Words: sEMG, Spatial features, Fuzzy Logic Controller

Chapter 1: Introduction

1.1 Problem Statement

There are over two million people with missing body limbs living in the United States based on National Limb Loss Information Center analysis [1]. The number of victims has been raising due to military engagements. By the year of 2050, this number will reach 3.6 million. There are still no prosthetic devices available which can mimic the full functionality of a human hand. Surface Electromyography (sEMG) is used in hand prostheses.

Being highly noisy, raw sEMG signals are very difficult to process. To address the problem, many controllers such as Fuzzy Logic Controllers, Adaptive Neuro-Fuzzy Inference Systems, Traditional Optimal Controller are being used in upper body prosthetic devices [2].

Heuristic Fuzzy Logic is used for EMG pattern recognition of multifunctional prosthesis control [3]. The membership functions are constructed by basic statistics tools- mean and standard deviation. Extensor digitorum, extensor carpi ulnaris, flexor digitorum superficialis, and flexor carpi ulnaris muscles are the four myoelectric control sites which are chosen to study. Four type of motions such as wrist extension, ulnar deviation, finger flexion, and wrist flexion are studied. Though it shows success in real-time recognition of state transitions, fuzzy controller does not do parallel control (i.e., multiple independent control motions).

Intelligent adaptive neuro- fuzzy inference system (ANFIS) based fuzzy Mamdani controller is used for a multifingered prosthetic hand [4]. The entropy values are used as inputs to design an ANFIS based fuzzy controller. The controller is designed to move the finger joint angles for grasping actions. The sensors are placed on ring, middle and index fingers. The model based position and force estimation are needed to be implemented. Nevertheless, the work on the controller to make a prosthetic hand more natural is still on going.

1.2 Literature Review

The history of Surface Electromyography development can be traced back to the mid 1600s. Francesco Redi first documented on electric ray fish that discovered a highly specialized muscle was the source of its energy [5]. Since then many developments have been done. Surface Electromyography becomes a popular solution for upper – limb deficiency such as unilateral transradial limb-deficiency, congenital limb-deficiency, etc.

Many control mechanisms such as Adaptive Neuro-Fuzzy Inference Systems and Traditional Optimal Controller have been introduced for these prosthetic hands; among them, Fuzzy logic controller is quite popular [6]. To identify motion commands for the control of a prosthetic hand, ANFIS is used where subtractive clustering algorithm has been developed to optimize the number of fuzzy rules. The back-propagation (BP) and least mean square (LMS) are used. Six movements such as hand opening and closing, wrist radial extension and flexion, pinch and thumb flexion are studied. However, the need for real-time analysis of control performance is growing.

1.3 Proposed Thesis Plan:

sEMG signals have played an important role for prosthetic device control. These signals are used for classification of human motions and its outcomes are fed to the prosthesis control system. The aim of this research is to develop a real-time fuzzy logic controller for motion identification using measured upper-body based sEMG signals. It is proposed to explore a spatial based classification method of sEMG signals in support of the temporal based classification algorithm generally used in order to infer intended human hand movements. For collecting the sEMG signals, a system with five surface sEMG electrodes are placed in a defined spatial pattern that

resembles a ring around the forearm. The proposed algorithm is accomplished using several steps.

First, an arrangement of five sEMG sensors equally distributed over the perimeter of the lower forearm of a human (healthy) subject is arranged. The corresponding sEMG signal measurements are recorded with their spatial coordinate information. The plot results into a pentagon – like shape whose angles change according to the signal strength of the measured sEMG signals. The data acquisition in real time is done using Matlab™. *Simulink*™ is used to visualize the real-time shape changing of the measurement pentagon. As a next step, a fuzzy inference system is developed using rules based on the resulting angles of the sEMG pentagon graph. The resulting fuzzy inference system is capable of controlling at least two movements- inner and outer forearm muscle movements. Finally, two movements are predicted by a fuzzy logic control mechanism.

Chapter 2: Background Information

The history of surface electromyography (sEMG) began with the interest of seeing things with the help of instruments which cannot be seen, felt, or touched with the normal senses such as electricity.

2.1 What are EMG Signals:

EMG means Electromyography. It is a process for evaluating and recording myoelectric signals produced by skeletal muscles. EMG signals are mainly two types: clinical and kinesiological EMG. Basically, neurologists and physiatrists use clinical EMG where as kinesiological EMG is prepared for literature considering movement analysis. Kinesiological EMG can be subdivided into two types: surface and fine wire. Both types have different advantages and disadvantages.

Surface EMG analysis gives a safe, easy, and noninvasive method that allows objective quantification of energy of the muscle [5]. There is no need to penetrate the skin to gain useful information regarding muscle movement. One can see the energy patterns which can't be seen with the naked eye. This method allows the observer to study muscle energy both at rest and changing of movement. The main drawback of sEMG signals is crosstalk. sEMG signals are distributed spatially. sEMG probes collect signals from other motor units which are stemming from different muscle groups. This phenomenon is known as crosstalk.

In contracts, fine wire is associated with needle insertion. When it comes to test small muscles, fine wire EMG gives better results than sEMG. Besides, it gives the ability to test deep muscle. The disadvantage of fine wire EMG is insertion of needles which is difficult to place the electrode repeatedly in the same area of muscle. For this work, sEMG is chosen due to its wide useful features.

2.2 How EMG Signals are Generated:

It is important to study muscle from a macroscopic level to a microscopic level to understand how EMG signals are generated. On a macroscopic point of view muscle is nothing but a group of fibers together; but in reality, muscle consists of different compartments. Figure 2.1 shows the details of muscle [7]. Each individual fiber can be broken down into clusters which are tiny hair-like stands known as Myofibrils. Each Myofibril is made from two types of filaments, and they are myosin and actin filaments.

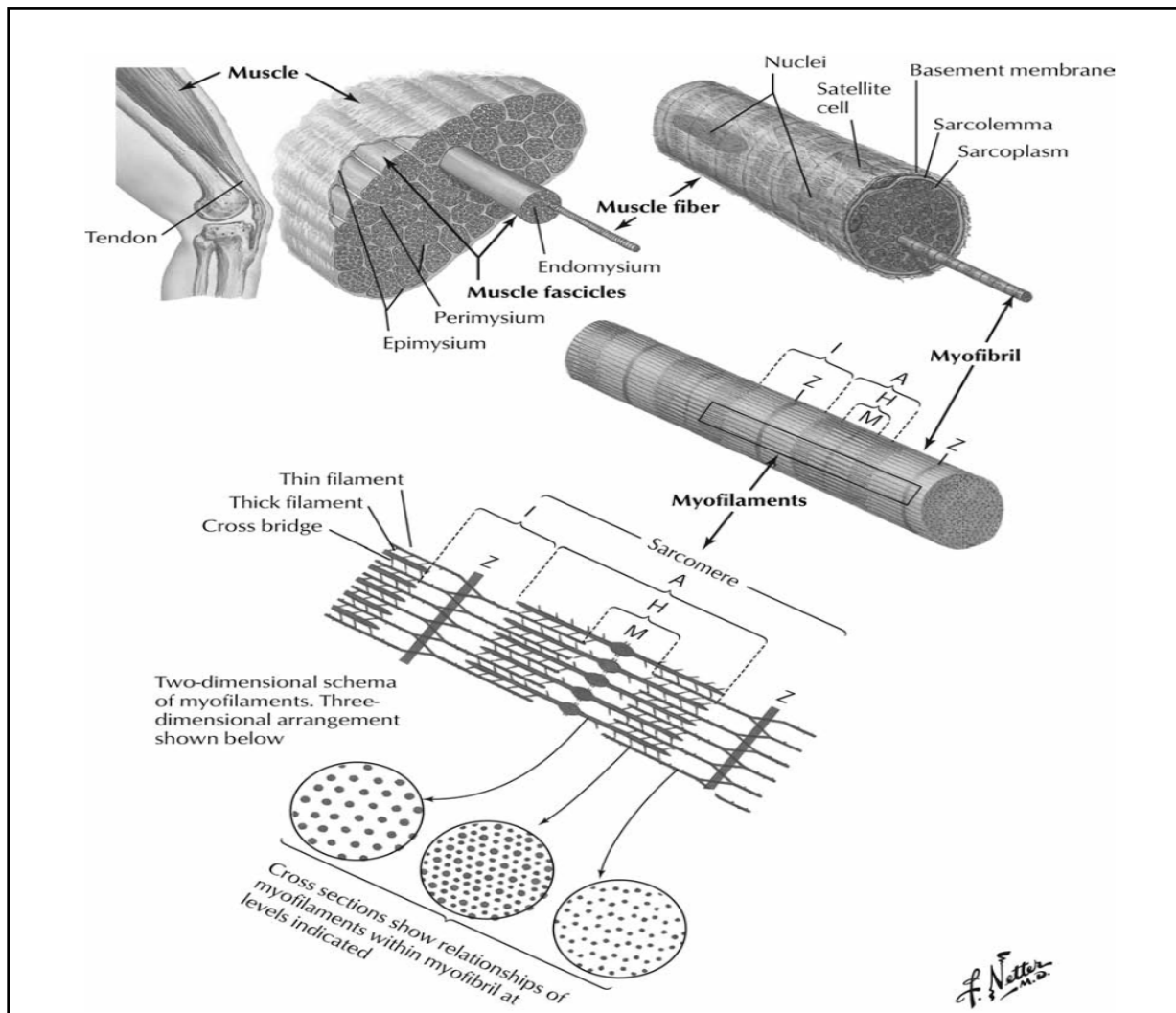


Figure 2.1: The composition of muscle cells, muscle fascicles, muscle fiber, myofibril, myofilaments, sarcomere, thick and thin filaments [7]

Then comes the nervous system organization of muscle where Motor Unit (MU) is the basic level. During muscle contraction EMG signals are generated by the simultaneous firing of several motor units. These motor units are the smallest functional element of the muscle contraction which creates EMG signals. There are mainly two parts of a motor unit which are motoneuron and muscle fibers. Figure 2.2 shows the parts of a motor unit [8]. Typically, each motoneuron innervates hundreds of muscle fibers.

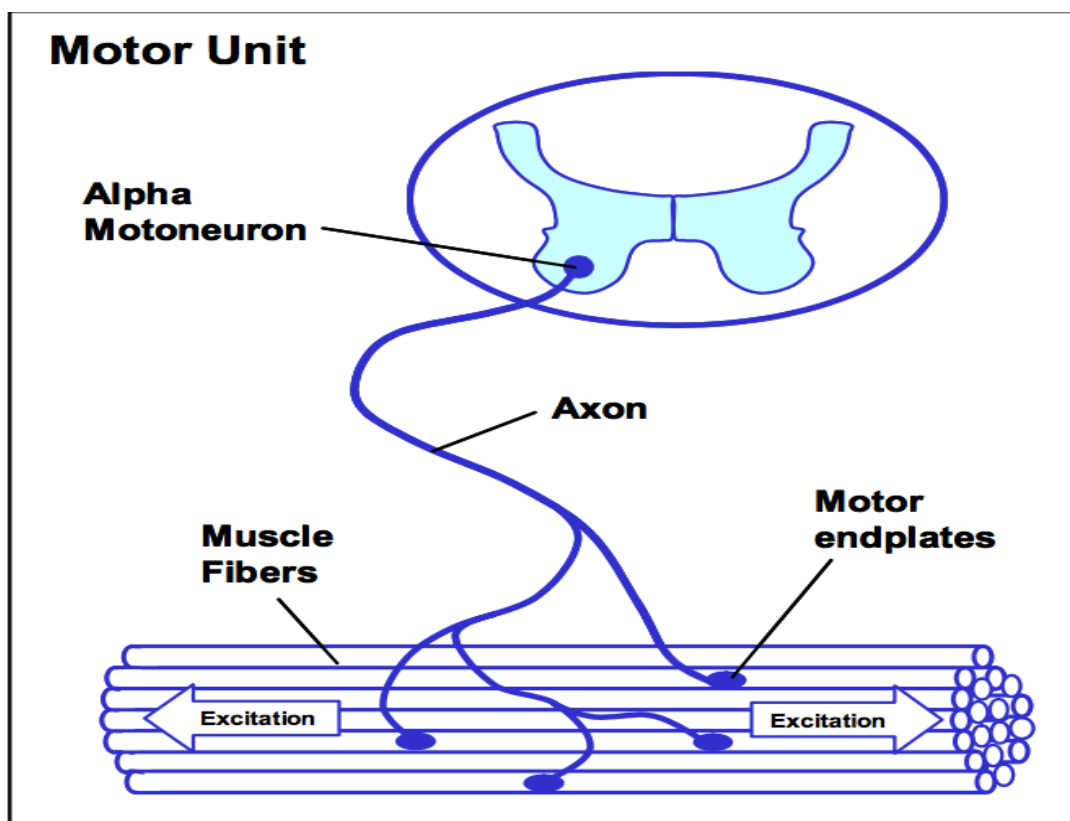


Figure 2.2: Parts of Motor Unit [8]

When muscle cells contract and relax, they produce electrical potential which can be detected by electromyography. Muscle filament sliding is triggered by an electrical phenomenon known as Action Potential (AP). This motor unit action potential is the source of sEMG. When the energy from the muscle reaches to the skin, it is collected by the electrodes.

2.3 Electrode Placement:

A pair of electrodes are required to record sEMG signals, because sEMG recording shows the potential difference between two separate electrodes. Electrodes work as tiny microphones which are used for listening to the muscles. Knowing where to place the electrodes is very important, because they pick up sEMG signals. According to Fridlund and Cacioppo, there are couple of elements to be considered before placing electrodes such as minimum amount of tissue between the electrodes and the muscle fibers, selecting appropriate position for the electrode with respect to muscle fibers, and so on [9]. In this work five electrodes are placed on lower forearm muscle equally distributed over the perimeter.

2.4 Where EMG used:

EMG are used in many sectors such as rehabilitation, medical research, sports science etc. EMG is one of the fast-growing sectors of medical science. There are more than 66 EMG instrument manufacturers existing in approximately 20 countries [7].

2.5 Classification Method for Feature Extraction:

The sEMG based pattern recognition requires feature extraction from the raw signals for performing classification. There are 3 types of features in EMG signal based control system. They are time domain, frequency domain, and time-frequency domain features. Time and frequency domain features are studied for this work. A spatial based classification is used for feature extraction. In frequency domain, the Fast Fourier Transform (FFT) is applied. For time domain analysis, the Standard Deviation (STD) and mean classifications are used. These classification methods are described below.

2.5.1 Standard Deviation

It is a time domain classification method. The Standard Deviation (STD) of a signal is used to measure how close the observations of a sample from the mean [13]. The STD can be expressed as below:

$$STD = \sqrt{\frac{1}{N-1} \sum_{i=1}^N |X_i - \mu|^2} \quad (1)$$

where, μ is the mean of the random variable, X

2.5.2 Mean

Mean is a common classification which is used to measure the central tendency of a random variable. Mean is defined by-

$$Mean = \frac{1}{N} \sum_{i=1}^N X_i \quad (2)$$

2.5.3 Fast Fourier Transform

The fast fourier transform is a part of fourier transform. It is a mathematical method which is used to transform a time domain function into frequency domain. Fourier transform can be expressed as:

$$\hat{f}(\xi) = \int_{-\infty}^{\infty} f(x) e^{-2\pi i x \xi} dx \quad (3)$$

for any real number ξ .

2.6 Fuzzy Inference System:

The history of fuzzy logic was started in the 19th century. The term fuzzy logic was first used in 1965 with the proposal of fuzzy set theory by Lotfi Zadeh [10]. Initially it was used to process data; later, it began to be considered as a control strategy. When it comes using human

knowledge for developing control system design, fuzzy inference system is preferable. Even fuzzy logic is used for real-time control system design.

The basic principle of fuzzy control system is assigning a particular output which depends on the probability of the state of input. It doesn't need perfect inputs rather a range of inputs would be sufficient. Fuzzy logic is used when partial truth between true and false values are needed to be calculated. In comparison with Boolean logic which has only two integer values 0 and 1, linguistic variables such as pressure, good, better etc. can be used in fuzzy logic system. With the help of fuzzy logic probabilistic features such as weather forecasting, restaurant review, etc. can be addressed.

Fuzzy works on the concept of sets. Some linguistic variables are defined by each set. Both possible state of the input and the degrees of change of the state are a part of the set. These sets are used for membership functions which are represented graphically. It works on simple if-else logic.

Chapter 3: Experimental Setup

The energy which is generated from muscle contract or relax has a small value and the value is measured in microvolt [5]. It is required to use some instruments to amplify the signals so that they can be seen for further processes. To collect meaningful EMG signals from the skin surface of a human subject, specific electrodes and signal processing methods are required. The whole process of collecting EMG signals is done in a circuit box. The box has three main circuit parts. All the three parts are explained below:

3.1 First Part: Instrumentation Amplifier

Instrumentation amplifiers are nothing but integrated circuits. They are very useful when dealing with low voltage situations. This differential amplifier is used to amplify sEMG signals. First, sEMG signal is fed to the non-inverting terminal of LM324 instrumentation amplifier. Then this differential input is multiplied by 100 to increase the strength of sEMG signal. Figure 3.1 shows schematic diagram of instrumentation amplifier.

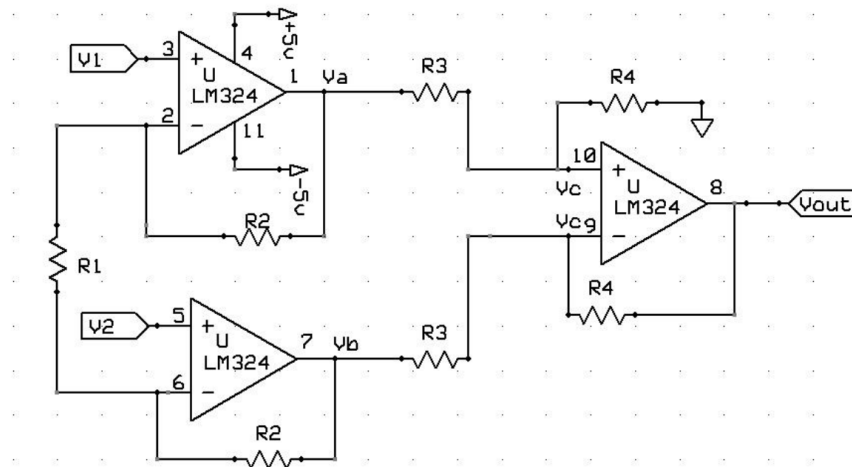


Figure 3.1: Schematic of instrumentation amplifier [11]

It has four resistors and three operational amplifiers. Operational amplifier (op amp) is a DC coupled high gain electronic voltage amplifier which has a differential input. The values of the registers are R1 - 2K Ω , R2 - 100 Ω , R3 – 10K Ω and R4 - 10K Ω . The values of variation from amplified output to input are ± 0.01 to ± 0.09 mV. After that, the amplified signals are fed to the notch filter.

3.2 Second Part: Notch Filter

A notch filter is considered as a band-stop filter with a narrow stopband. It blocks all frequencies that fall within its bandwidth. Notch filter removes the noise caused by electronic parts such as power supply [11]. Notch filter consists of a low and high pass filter and an amplifier. The circuit is designed in such a manner that the cut-off frequency assigned by a high-pass filter is greater in value as compared to a low-pass filter. Thus, the difference between those two cut-off frequencies represent the bandwidth of the filter. Figure 3.2 shows notch filter.

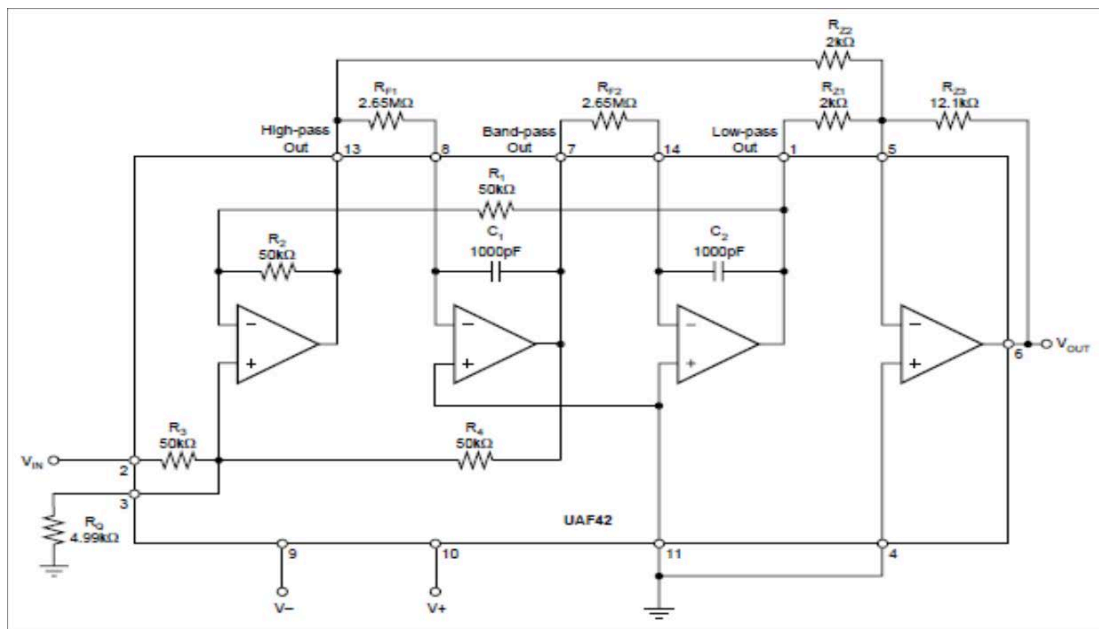


Figure 3.2: Schematic diagram of notch filter [11]

The assigned values of the resistors are $R_q - 4.99\text{K}\Omega$, R_{F1} and $R_{F2} - 2.65\text{ M}\Omega$, $R_{Z3} - 12.1\text{K}\Omega$.

Then the output from notch filter is fed to bandpass filter.

3.3 Third Part: Passband Filter

For this work, a Chebyshev type II 0.1dB passband is used. Chebyshev is named after Pafnuty Lvovich Chebyshev who is a Russian mathematician [12]. This filter is used to separate frequencies of one band from another. It eliminates the error in between the actual and idealized filter. Chebyshev type II consists of both high-pass and low-pass filters. Figure 3.4 shows a high-pass filter designed for frequency 450Hz.

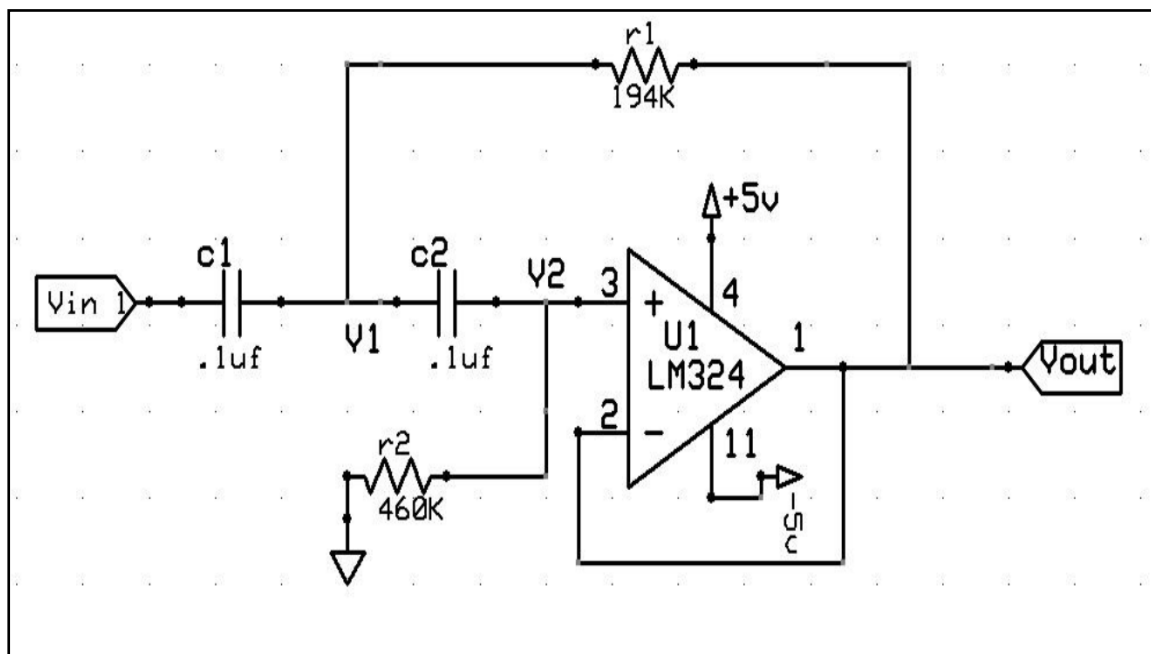


Figure 3.3: Schematic diagram of high-pass filter [11]

The output from a high-pass filter passes through a 4Hz low-pass filter. Figure 4.5 shows a low-pass filter.

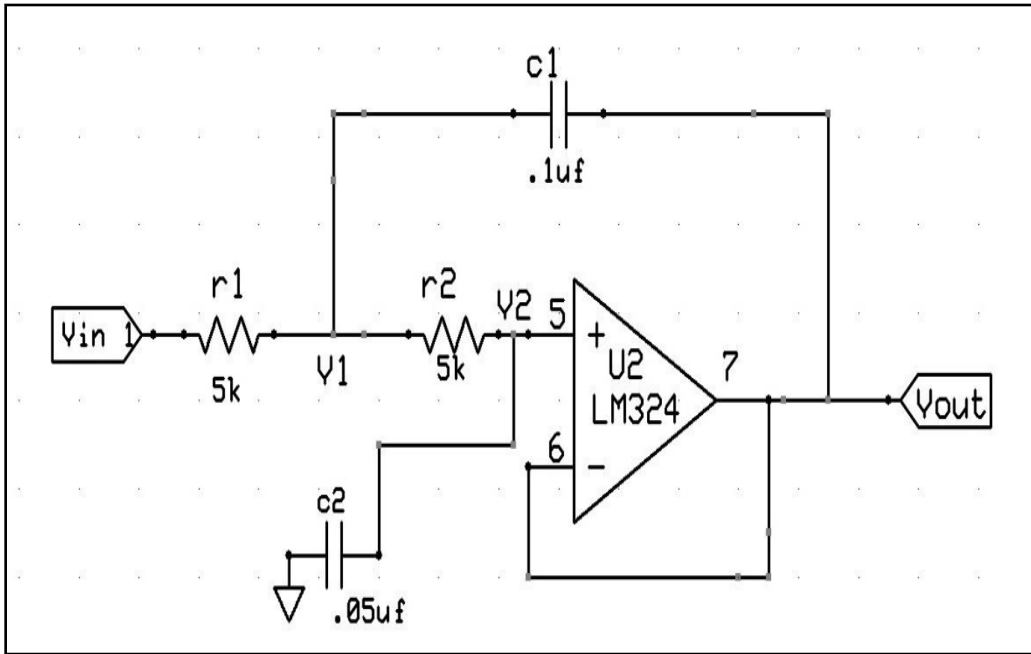


Figure 3.4: Schematic diagram of low-pass filter [11]

The output range of a low-pass filter is from $\pm 0.01V$ to $\pm 0.09V$ which is the final step to achieve sEMG signal. This output value is not enough to measure regulate-voltage and the reason is Arduino. Buffer amplifier is required to amplify the signal. The voltage buffer amplifier is used.

Figure 3.5 shows a voltage buffer amplifier where the values of the registers are R1 & R3 - $2K\Omega$, R2 - $27K\Omega$, R4 & R5 - $33K\Omega$, R6 - $10K\Omega$.

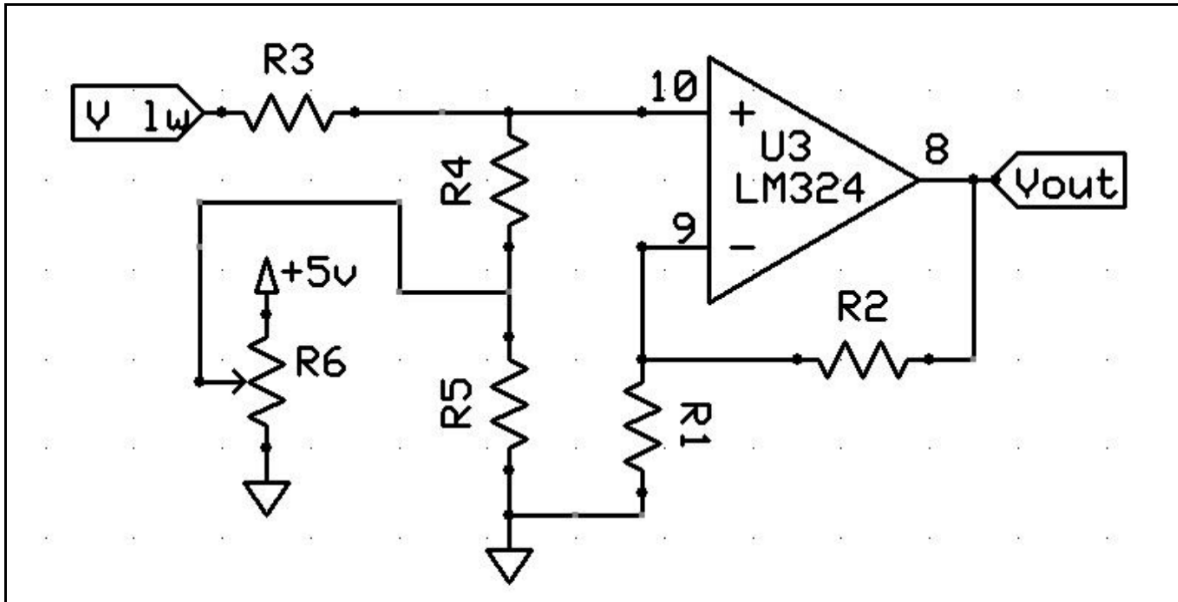


Figure 3.5: Schematic diagram of voltage buffer amplifier [11]

All the circuits are implemented into a PCB (Printed Circuit Board). Figure 3.6 shows a model PCB. This PCB needs $\pm 5V$ power supply from a battery. Both the power supply circuit diagram and connection are shown in figure 3.7 and 3.8. The values of the regulators are U3 10V, U1 and U2 $\pm 5V$. An approximately 23V is supplied from an old laptop lithium -ion batteries.

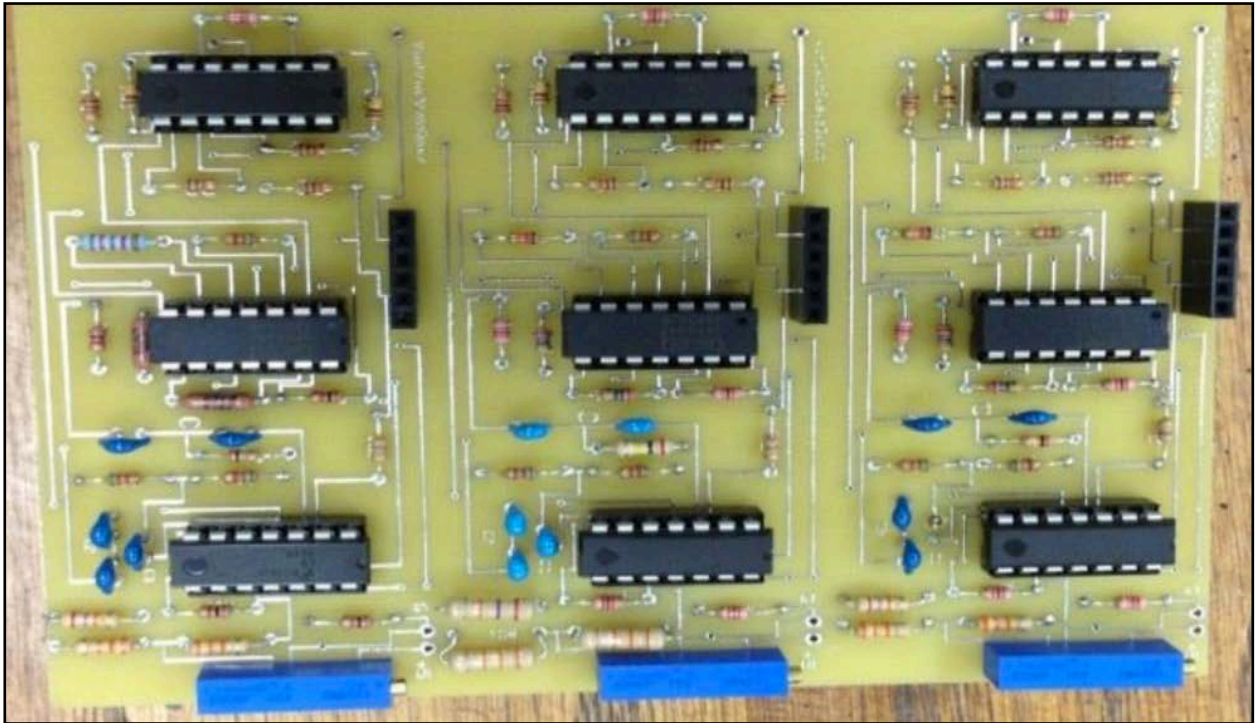


Figure 3.6: A Printed Circuit Board model [11]

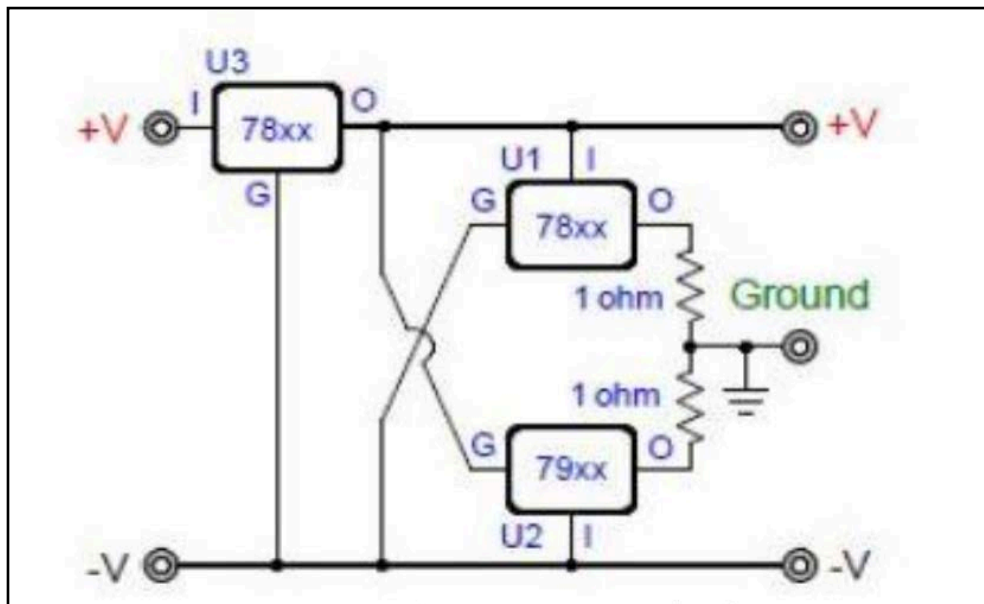


Figure 3.7: Schematic diagram of power supply [13]

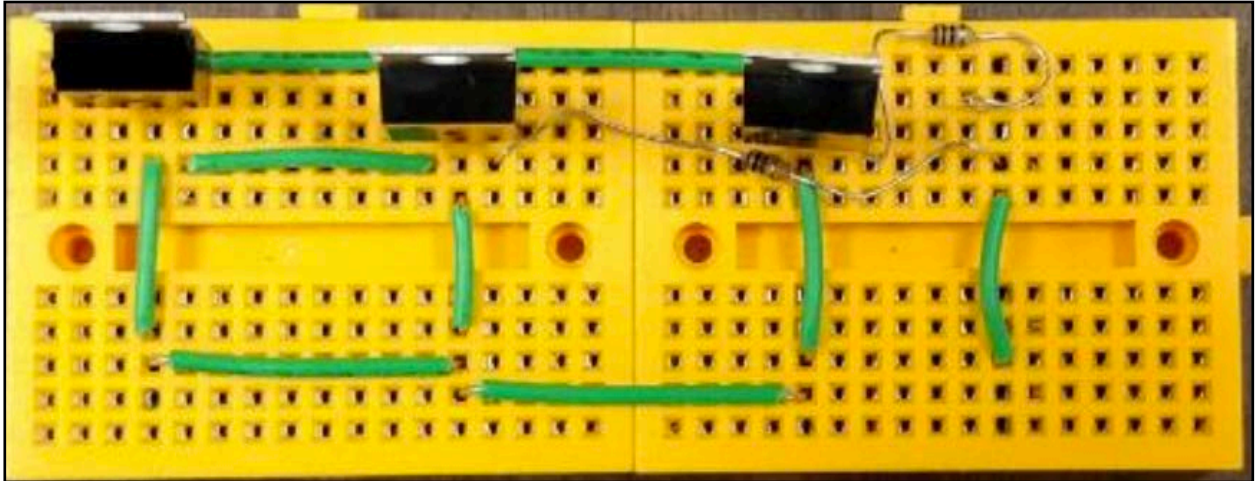


Figure 3.8: Circuit connection of power supply [13]

3.4 Shortcomings

The channel box had some issues regarding collecting sEMG signals. The box has ten channels which are shown in figure 3.9. Five channels from them are in placed in right side of the box, and other five channels are placed in left side of the box. Sometimes sEMG signals from ten channels shown some noise. To solve the noise problem, some additional tasks were done.

The box had only one power supply. One additional power supply was added to the box in such a way, so that one power supply will work for right sided five channels, and another power supply will cover the left sided five channels. Still, the sEMG signals were noisy. After checking the connections, it was found that box had ground connection issues. Besides, the electrodes which were connected to the PCB through poles, were creating noisy signals. To address the problem, a new power supply was built by using the solderable breadboard. This gives a robust ground connection.

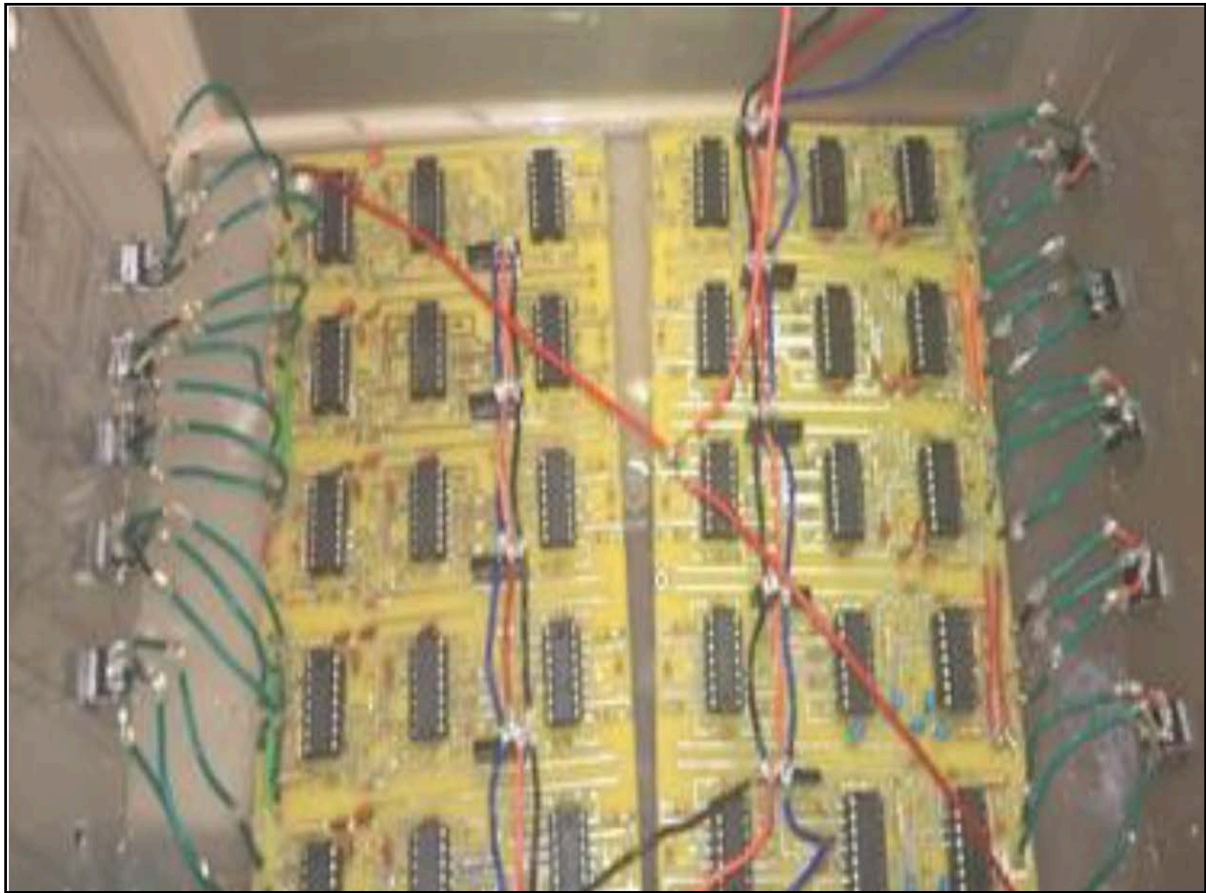


Figure 3.9: Ten channels sEMG box [13]

Figure 3.10 shows new power supply of solderable board with connections. After that, the poles on the sensor board had been removed. Then, the electrodes were directly connected to the PCB by soldering. The final modified box is shown in figure 3.11. The solderable board power (red color) supply was placed at left side of the box. The right sided five channels were connected to bread board (white color) power supply. As, there wasn't any ground issue at right side of the box, the poles and power supply on right side didn't change.

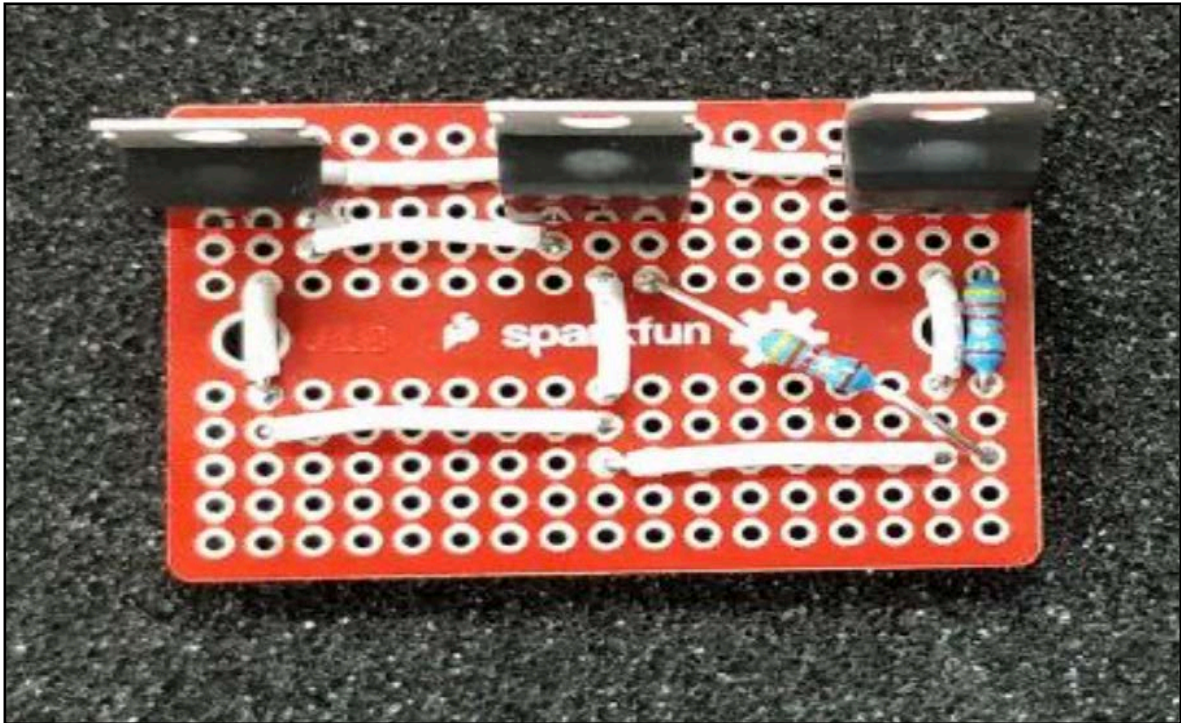


Figure 3.10: A new power supply of solderable board with connection [13].

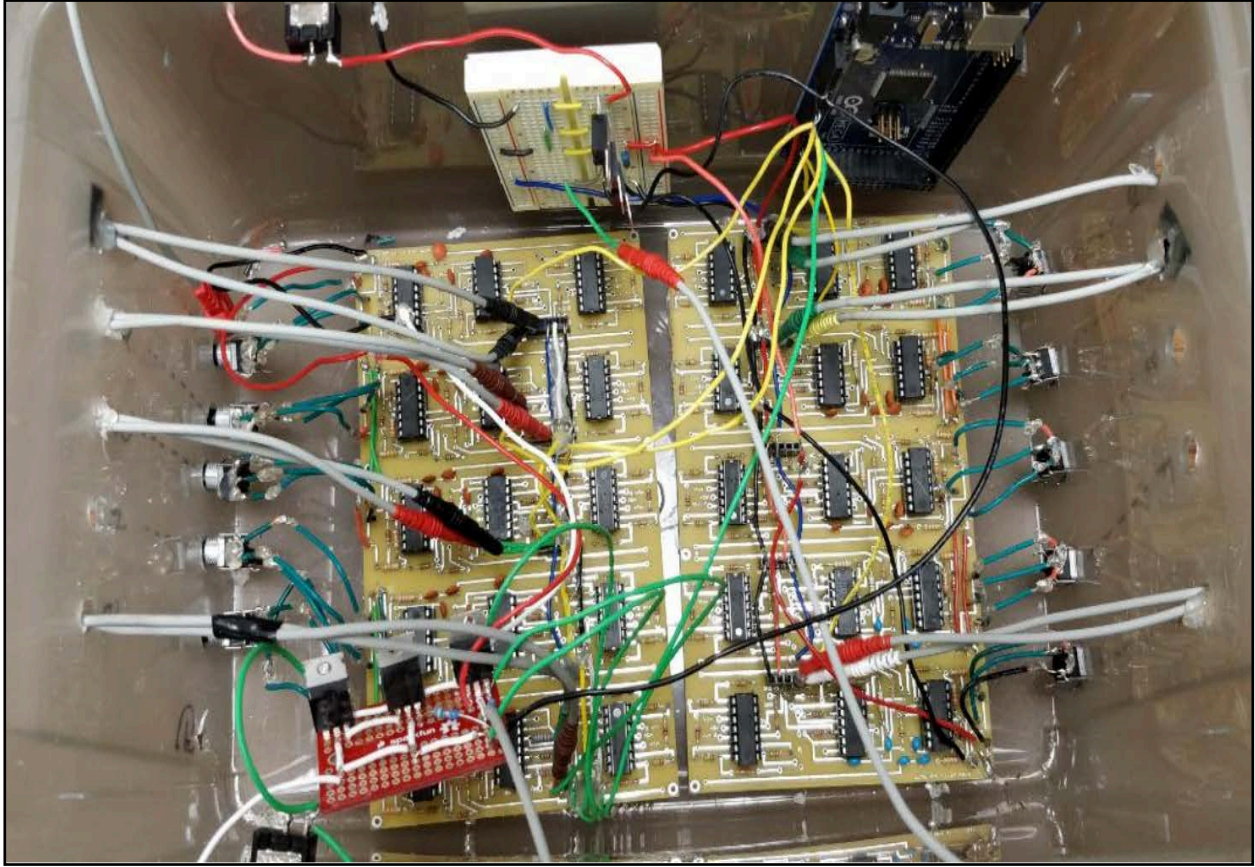


Figure 3.11: Final sEMG box with connections [13]

3.5 Placement of Electrodes:

After confirming the proper circuit connection and the right position of electrodes on forearm, the sEMG signals can be produced by forearm muscle movements. Figure 3.12 and Figure 3.13 shows how the two hand motions should be performed. A *Simulink*TM model described in the Appendix is used to produce sEMG signals with the two forearm muscle movements. Figure 3.14 and Figure 3.15 shows the outputs of the two motions.

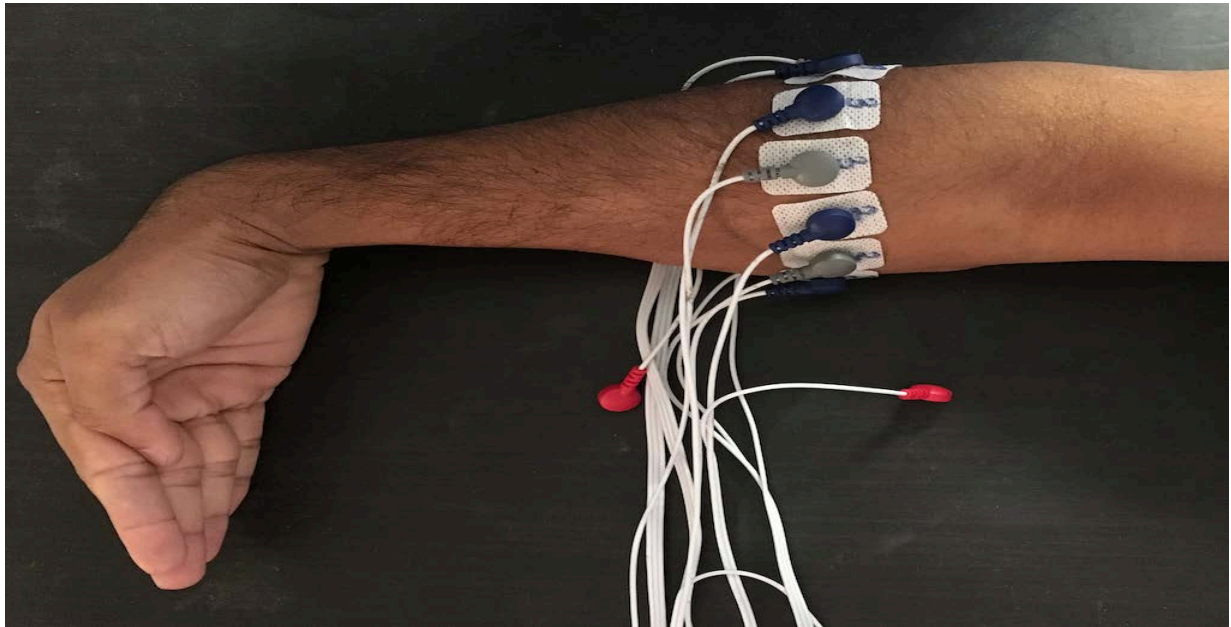


Figure 3.12: Inner forearm muscle movement position



Figure 3.13: Outer forearm muscle movement position

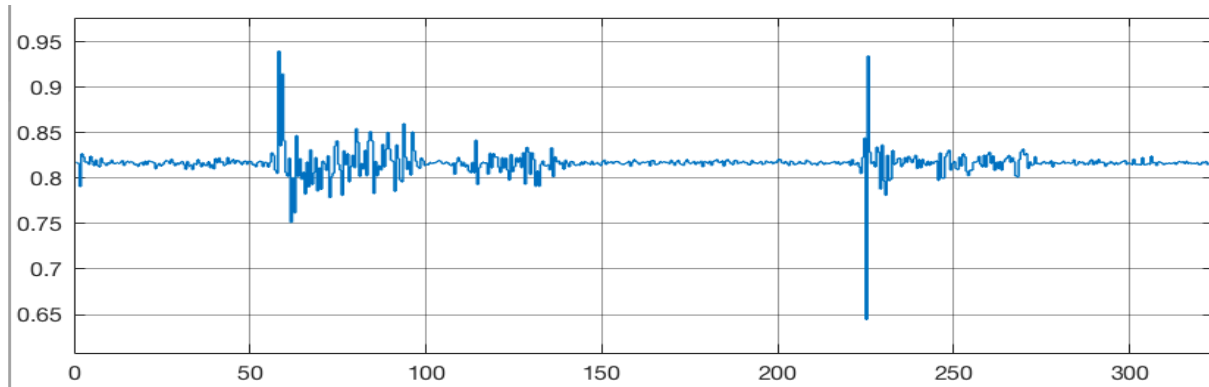


Figure 3.14: sEMG signals for the inner forearm muscle movement

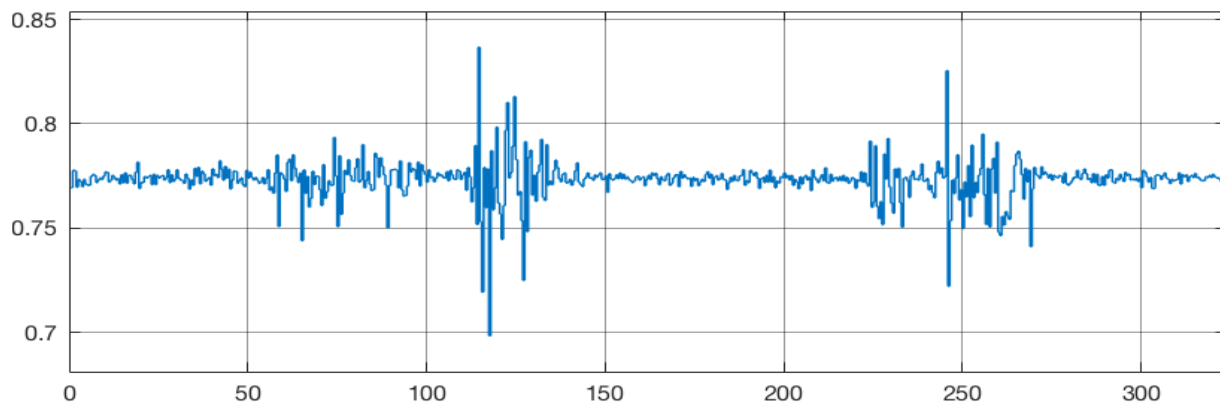


Figure 3.15: sEMG signals for the outer forearm muscle movement

From Figure 3.14 and 3.15 it can be said that two sEMG signals have opposite pattern as the inner and outer forearm muscle movements contradict each other movement position.

Chapter 4: Methodology/Proposed Design

4.1 Overview:

To make use of the spatial properties of sEMG signals, a specific arrangement of the sensors is proposed. In particular, the idea is to place five sEMG sensors around the forearm in a ring shape. Data from each sensor is considered as an axis. The equal distribution of five axes gives a pentagon shape and a polar chart is utilized. Each raw signal is recorded and graphed as a height on the polar chart axis. When all heights are connected, it gives a five-sided polygon (pentagon). The process from spatial visualization to motion prediction by fuzzy logic in real-time is done in two parts: visualizing the change of the shape of the pentagon and developing a fuzzy logic controller based on the sEMG classification.

4.2 Visualizing the Change of the Shape of the Pentagon:

Five arbitrary values of radius are taken, which are placed as a height in a polar chart. A geometric circle is considered to place five sEMG sensors equally over the perimeter of the circle. Figure 4.1 shows the polar plot.

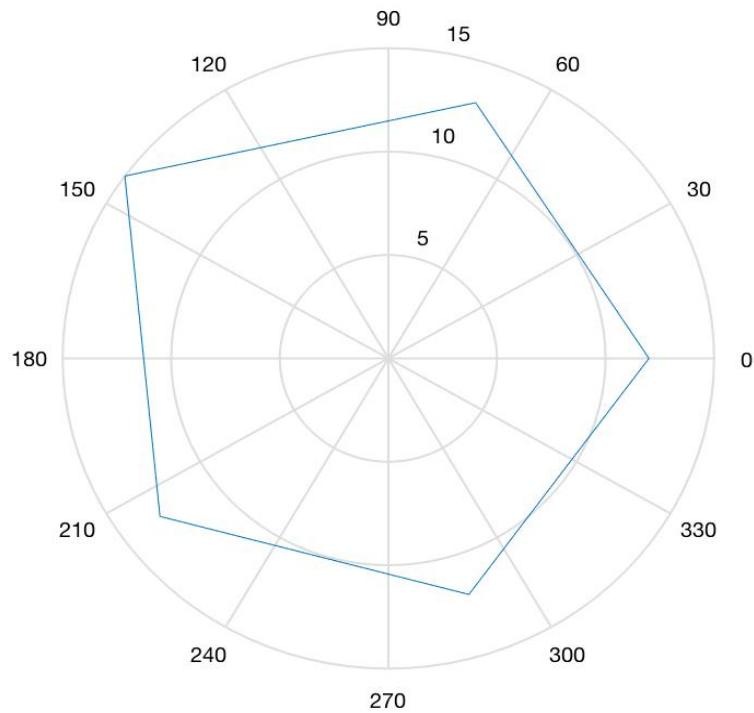


Figure 4.1: Polar plot of five channels equally distributed with arbitrary radius value

Five arbitrary values of 12, 13, 15, 13, and 12 are chosen as radii. Those values are placed along the axis of the circle. The angle between any two radii is 72, because the circle is equally divided by those five radii. Each height of arbitrary value along the circle axis and the equally distributed angle (72 degree) make a point on the polar chart. When the five points are connected, it gives a geometric pentagon shape. This pentagon shape is important for visualization. Features of sEMG signals can be extracted after the visualization of shape changing of the pentagon. To see how the pentagon shape is changing, another set of arbitrary radii values are chosen. The values are 5, 13, 13, 16, 6, and 5. The new pentagon is plotted on the same graph over the previous pentagon. Figure 4.2 shows the overlapping.

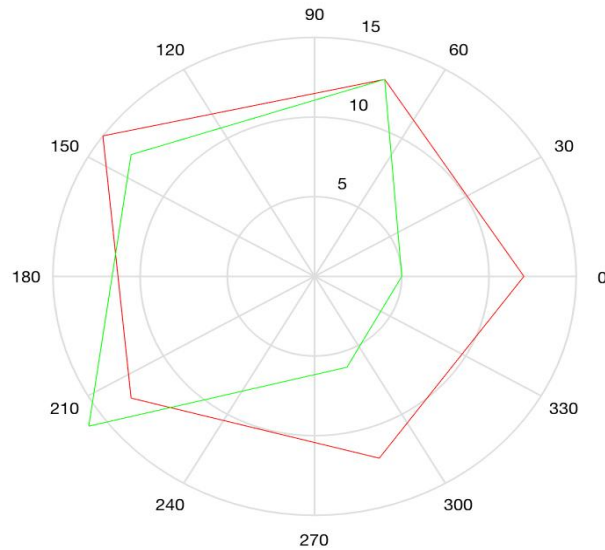


Figure 4.2: Overlapping of two sets of arbitrary values

The big pentagon (red color) represents the first set of arbitrary values and the small pentagon (green color) represents the second set of arbitrary values. It is required to see the continuous shape changing. To see the continuous shape changing of the pentagon, a *SimulinkTM* is used. Figure 4.3 as described in the Appendix shows the *SimulinkTM* model. The five arbitrary sine waves are used as inputs. A *MatlabTM* user defined function as described in the Appendix contains the code for calculating the area and plotting the pentagon shape. In *MatlabTM* function block u_1, u_2, u_3, u_4 and u_5 are defined as inputs. Those inputs are considered as radii of the circle. *Polar* command is used in *MatlabTM* to plot the pentagon.

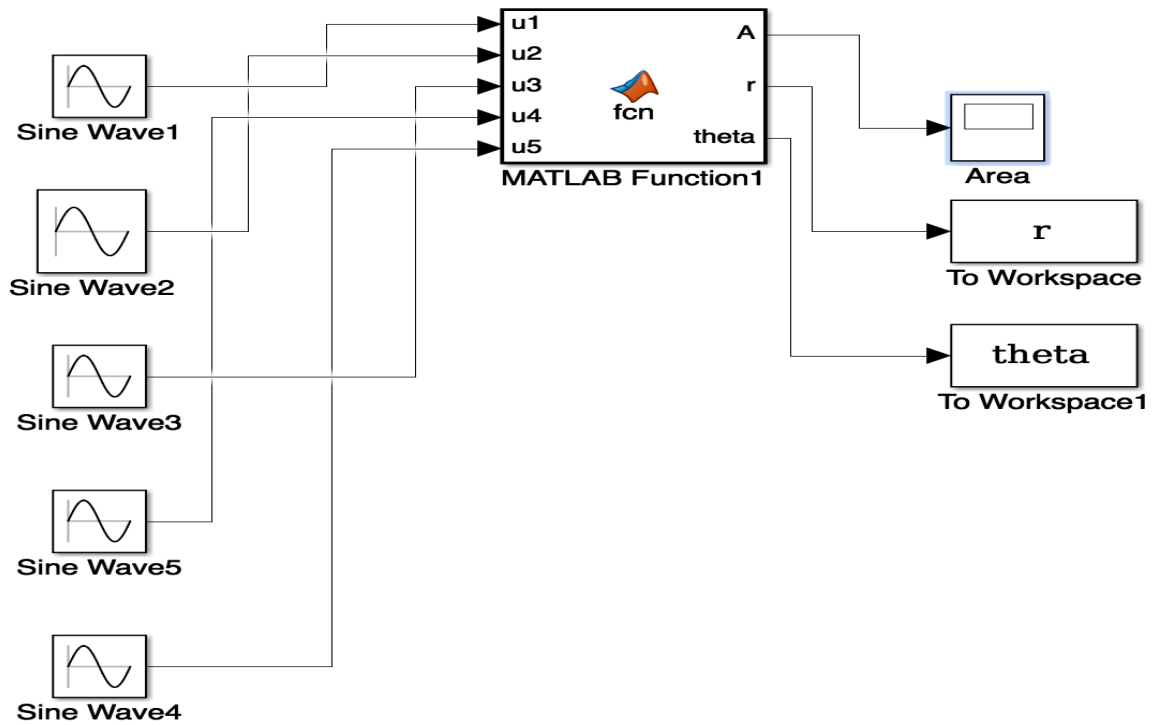


Figure 4.3: *SimulinkTM of five arbitrary sine waves to get visualization of continuous shape changing*

Analog input blocks are used in a *SimulinkTM* model to see the real-time shape changing of the pentagon. Figure 4.4 as described in the Appendix shows the *SimulinkTM* model. The collected inputs from analog inputs are converted into readable outputs. The data type conversions are done by the block next to the analog input blocks (figure 4.4).

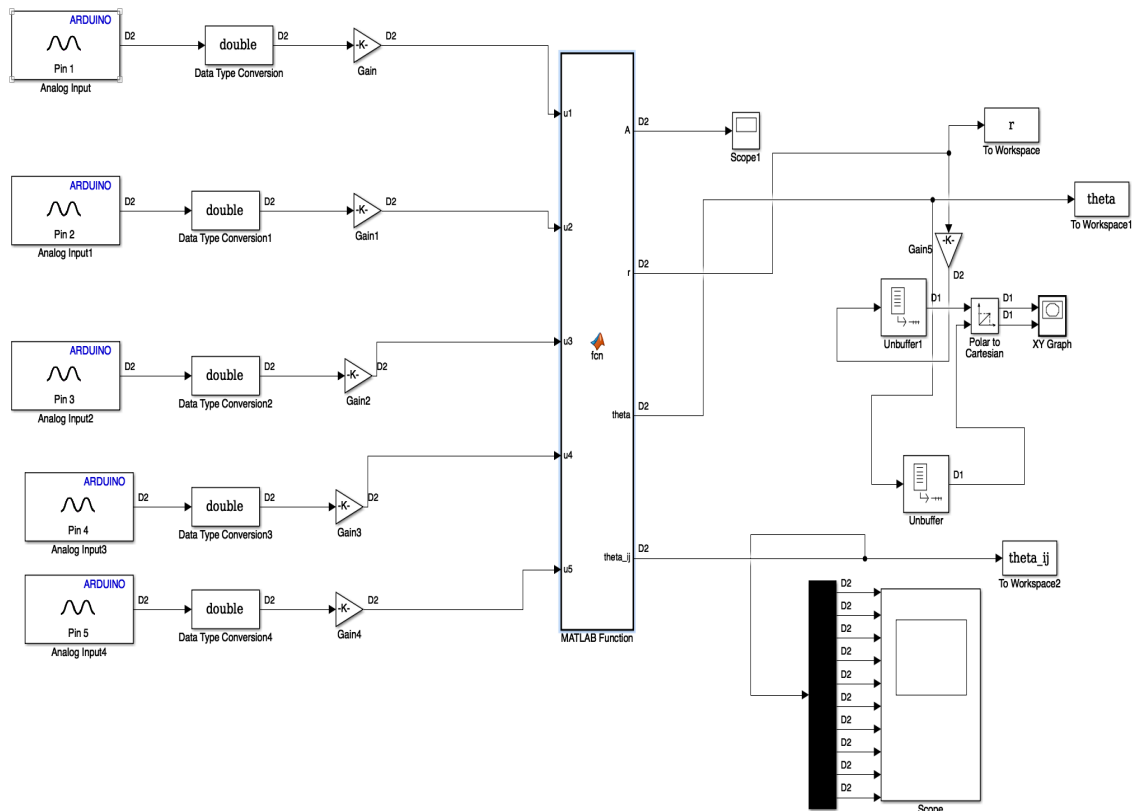


Figure 4.4: Using analog inputs in SimulinkTM block to get internal ten angles of the pentagon

Ten internal angles of the pentagon are required to calculate for extracting sEMG features. Figure 4.5 shows a Schematic diagram of a pentagon. It has ten internal angles from θ_{12} to θ_{15} . An algorithm is needed to calculate those angles. The angle between r_1 and r_2 is 72° . This angle with θ_{12} and θ_{21} make a triangle (Figure 4.6). Simple trigonometric sine rules are used.

$$\frac{\sin a}{A} = \frac{\sin b}{B} = \frac{\sin c}{C} \quad (4)$$

Here, A, B, and C represent arms of a triangle and a, b, and c are angles opposite to the arms.

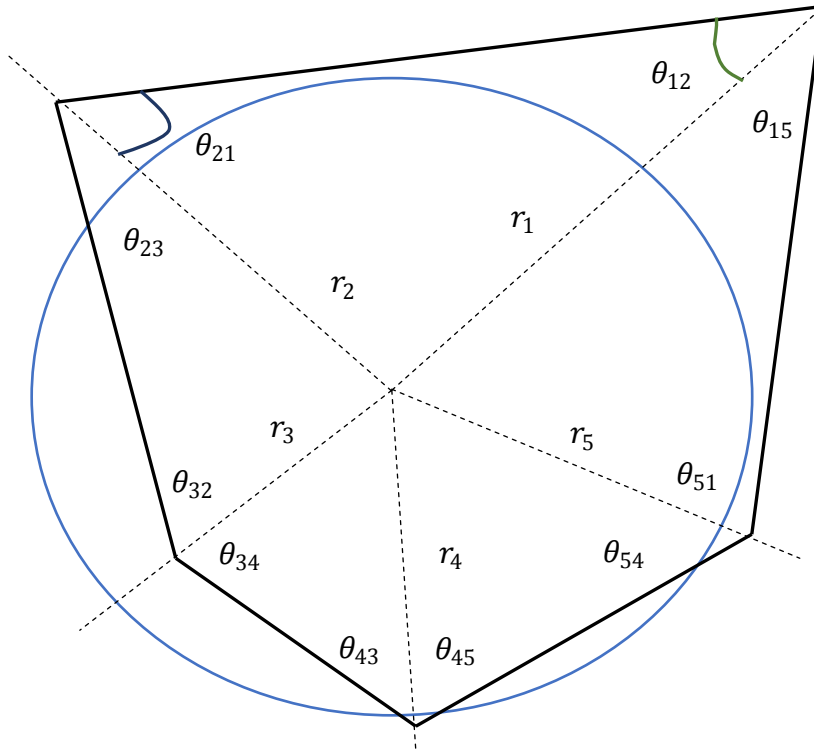


Figure 4.5: Schematic diagram of a pentagon

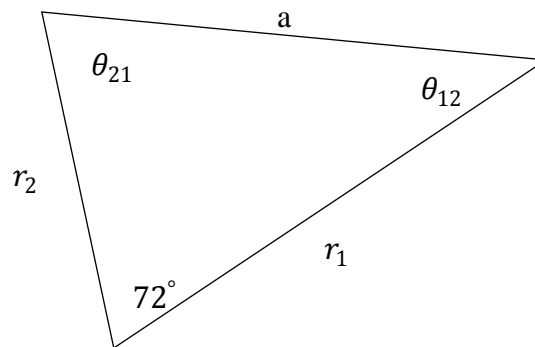


Figure 4.6: Part of a pentagon

From figure 4.6 the following equation can be written:

$$\theta_{12} = \sin^{-1}\left(\frac{r_2}{a} \sin 72\right) \text{ and } \theta_{21} = \sin^{-1}\left(\frac{r_1}{a} \sin 72\right) \quad (5)$$

therefore, $a = \sqrt{r_1^2 + r_2^2 - 2r_1r_2 \cos 72}$. Using the value of a , θ_{12} and θ_{21} are calculated. The values of ten internal angles are studied to develop a fuzzy inference system.

4.3 Developing a Fuzzy Inference System:

A fuzzy logic controller has four parts. They are inputs-outputs, membership functions, fuzzy logic, and simulation. Linguistic variables such as temperature, taste of a food, etc. can be chosen as inputs for fuzzy logic. Fuzzy logic works on a range of inputs. Unlike Boolean logic, fuzzy logic doesn't depend on two integer values (0 and 1). The FFT, STD, and mean classification methods are used on sEMG signals to select the inputs and outputs for a fuzzy inference system. The data of STD classification method on the two internal angles as described in Chapter 5 is used for developing a fuzzy logic controller.

4.3.1 Defining Inputs and Outputs

The first step for developing a fuzzy logic controller is assigning values to input and output variables. For this work, two inputs and three outputs are used. The inputs are θ_{12} and θ_{34} as described in Chapter 5. Motion is defined as output in fuzzy inference system. The inner and outer forearm muscle movements have three stages. They are inner forearm muscle movement, rest position, and outer forearm muscle movement. These three stages of movements are considered for the outputs of the fuzzy logic controller and they are defined as LOW, MEDIUM, and HIGH. Two membership functions defined as LOW and HIGH are used for both inputs. Gaussian curve membership functions (gaussmf) are chosen for both inputs. For θ_{12} as described in Chapter 5, the range of LOW and HIGH membership functions is from 0 to 0.07. For θ_{34} , the range of LOW and HIGH membership functions is 0 to 0.035. Trapezoidal shape membership

function (trapmf) is chosen for the output. The ranges of three membership functions of the outputs are the same and it was from 0 to 1.

4.3.2 Fuzzy Rules and Fuzzy Reasoning

Fuzzy logic can be developed based on linguistic variables such as “LOW”, “MEDIUM”, “HIGH” and these can also be computed mathematically. Based on this idea, the fuzzy rules can be developed with a series of IF...THEN rules. The following rules were developed for the fuzzy logic controller.

- 1. If theta 12 is LOW and theta 34 is LOW, then motion is MEDIUM*
- 2. If theta 12 is HIGH and theta 34 is LOW, then motion is LOW*
- 3. If theta 12 is LOW and theta 34 is HIGH, then motion is HIGH*
- 4. If theta 12 is HIGH and theta 34 is HIGH, then motion is MEDIUM*

Figure 4.7 shows the max-min relationship graphically for the above rule no. 1. Figure 4.7 can be described as follows:

If theta12 and theta 34 are defined by the fuzzy membership function as LOW and HIGH respectively, then the output membership function can be defined as MEDIUM. The remaining fuzzy rule sets (from rule 2 to rule 4)are graphically shown in Figure 4.8.

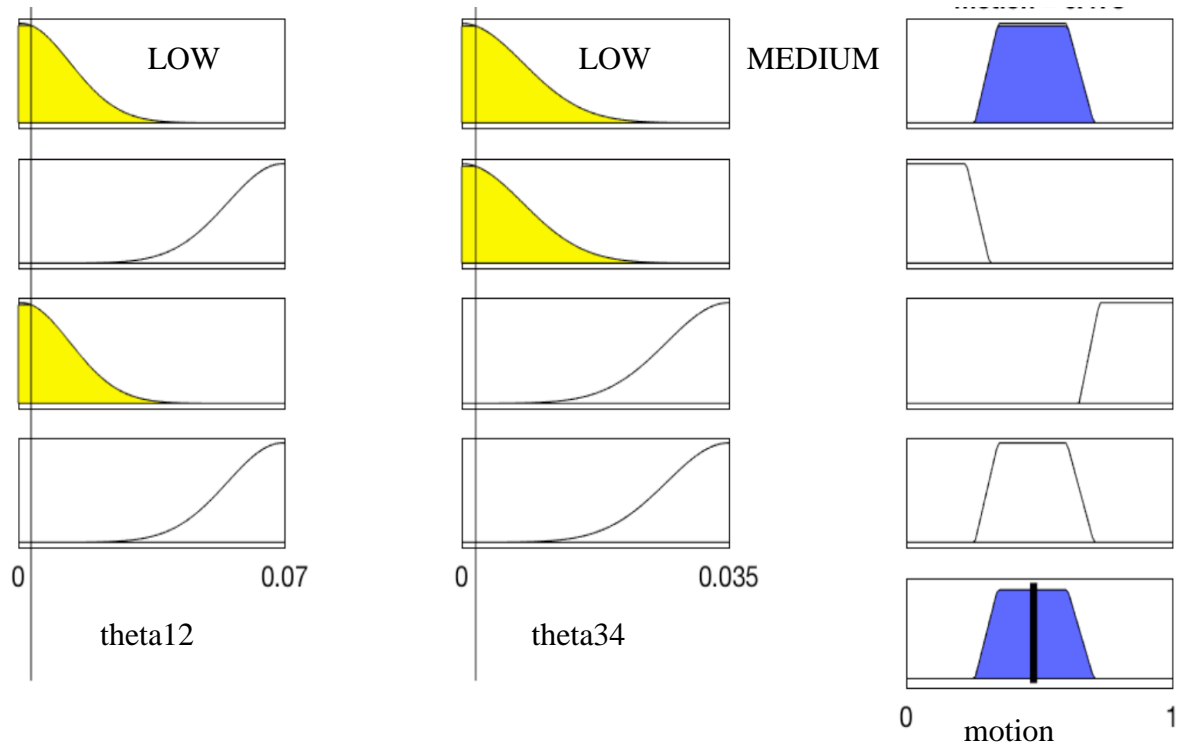
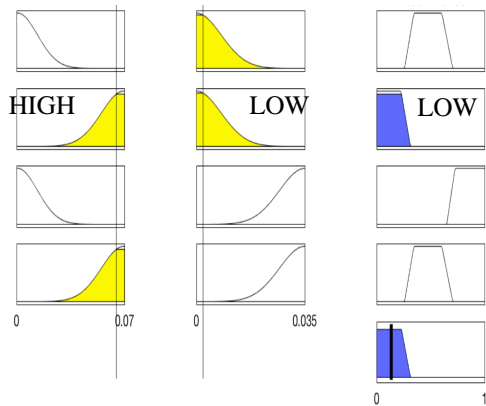
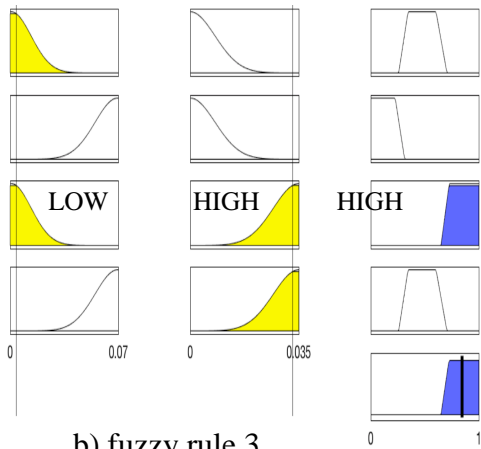


Figure 4.7: MF reasoning using fuzzy max-min decomposition (fuzzy rule no.1)

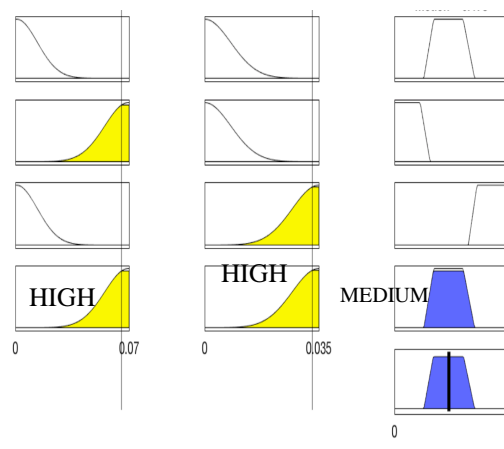


left column- theta12 (LOW/HIGH)
middle column- theta34 (LOW/HIGH)
right column- motion (LOW/HIGH/MEDIUM)

a) fuzzy rule 2



b) fuzzy rule 3



c) fuzzy rule 4

Figure 4.8: MF reasoning using fuzzy max-min decomposition (fuzzy rules no. 2,3,and 4)

4.3.3MF Defuzzification

The control devices such as actuator, servos, etc. require crisp value as their input. For that purpose, defuzzification is used in the fuzzy inference system. The Centroid of Area (COA) defuzzification method is used for this work [14].

Chapter 5: Discussion and Result

The entire experiment can be discussed in three main parts. They are spatial based visualization of shape changing of a pentagon, development of a fuzzy inference system, and identification of motions. The three main parts are discussed below.

5.1 Spatial Based Visualization of Shape Changing of a Pentagon

It is important to visualize how a spatial based shape is changing in real time when any simple human forearm motion is given, so that, useful features of sEMG can be extracted. Here, the goal is to combine five equally distributed sEMG sensors along with the axes of a circle so a pentagon shape is created. The shape of the pentagon is changed when different sEMG signals with different magnitudes are collected. First in *MatlabTM*, a polar plot of five arbitrary values equally distributed over the perimeter of a circle is created. These five radii and equally distributed angles create a pentagon. Another set of arbitrary values are used for overlapping on the same polar plot to visualize the shape changing. Different shapes of a pentagon give different areas. Cartesian coordinates are required to calculate those areas in *MatlabTM* because area in polar plot is difficult for visualization. *MatlabTM* has *polyarea* command for this purpose.

A simulation was required for visualization of continuous shape changing as the experiment is done in real-time. Five arbitrary sine waves are used for the simulation. This gives a visualization of continuous shape changing. After that, an Arduino microcontroller is connected to see the real-time shape changing with respect to sEMG signals. The shape changing is shown in a Cartesian plot. This visualization helps to extract features from the sEMG data, so that a fuzzy inference system can be built to identify human motion.

5.2 Development of a Fuzzy Inference System

After visualization of a pentagon shape changing, a fuzzy inference system is created in order to identify human arm motions. Some distinct features of sEMG signals are utilized to build a fuzzy inference system. To find those distinct features, both the areas and angles of the pentagon are studied.

The sEMG signals are generated during the forearm movements. Two movements of forearm are used here. They are inner and outer forearm muscle movements. Then, the pentagon shape created by those movements are studied. To extract useful features from the area of the pentagon, different types of classification methods, such as Standard Deviation (STD), Fast Fourier Transfer (FFT), etc. can be applied on this data. Chapter4 describes how the area is computed.

The goal is to see how the area varies during the forearm movements as described in chapter 4. To measure that variation, a STD classification is used on the instantaneously captured area. Figure 5.1 shows the output graph of the Standard Deviation classification on the captured area of the pentagon. The peak at the very beginning of the graph is caused by additional noise from channels which is associated before the forearm movements are started. After that, the graph shows some deviations from the mean value. These values are associated with forearm movements.

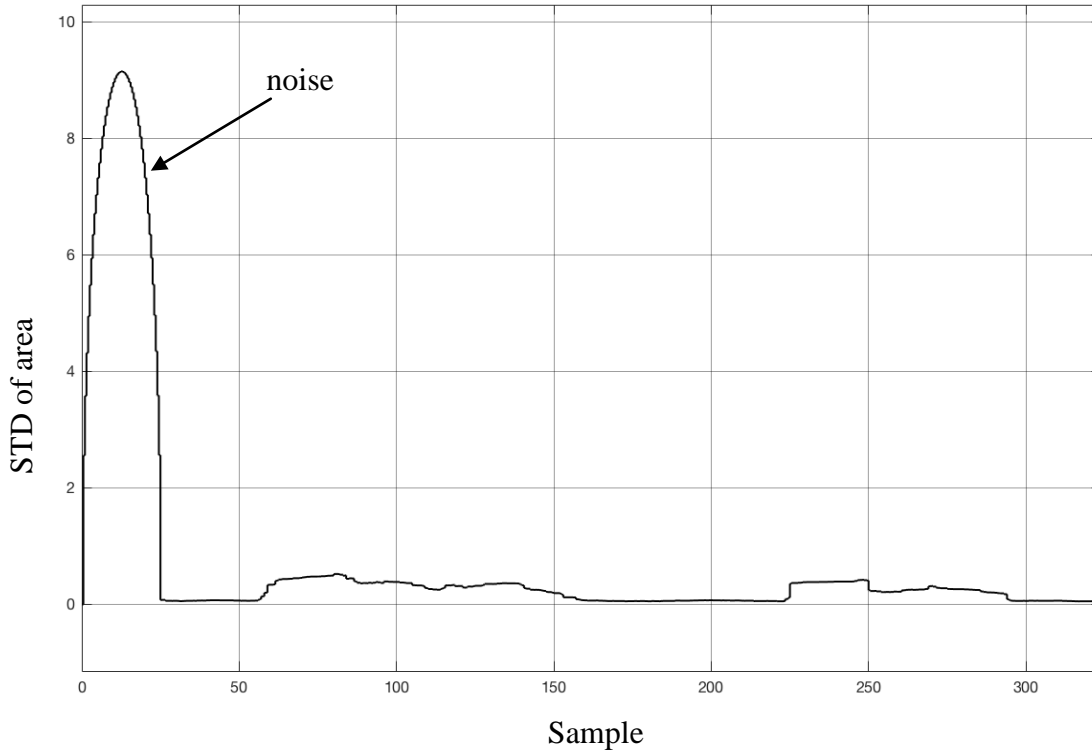


Figure 5.1: Output graph of STD classification on area

Figure 5.2 gives a closer view of the forearm muscle movements of the same graph (Figure 5.1). The samples approximately from 60 seconds to 70 seconds (section 1 in Figure 5.2) are associated with inner forearm muscle movement and the samples approximately from 71 seconds to 120 seconds (section 2 in Figure 5.2) are associated with resting position of the forearm muscle. Samples approximately from 121 seconds to 155 seconds (section 3 in Figure 5.2) represent outer forearm muscle movement. This sequential inner, rest, and outer forearm movements followed by up to sample 350 seconds (Figure 5.2).

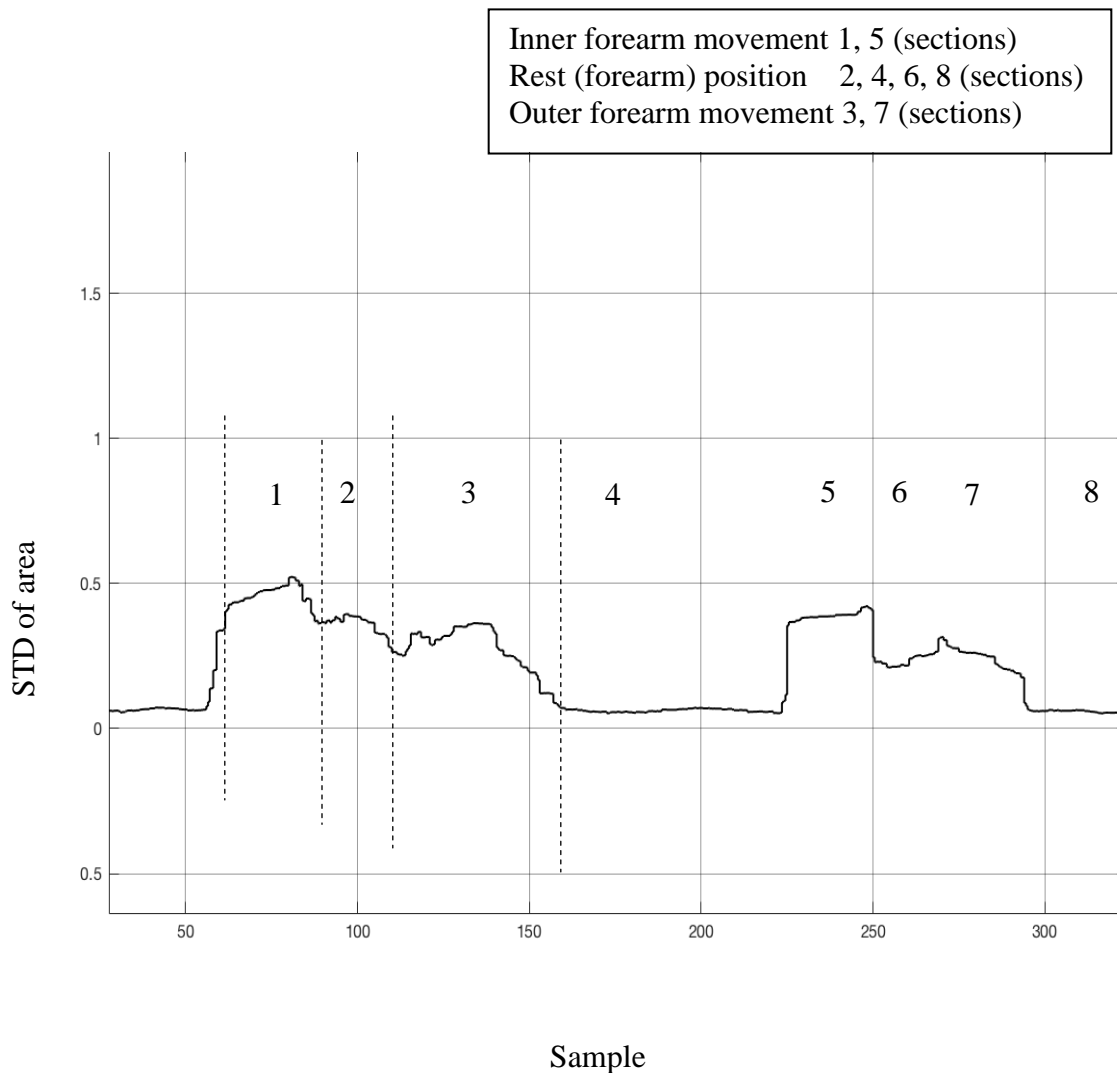


Figure 5.2: Output graph of STD classification on area (closer view)

To find more useful information for identifying the forearm muscle movements, another classification, the FFT, is applied on the area data. Figure 5.3 shows the output graph of the FFT classification with respect to the forearm movements. It shows some noise at the beginning which is similar to Figure 5.1. This is due to the same additional noise from the initiation of the experiment. After that, it shows some very noisy overlapping responses associated with forearm movements.

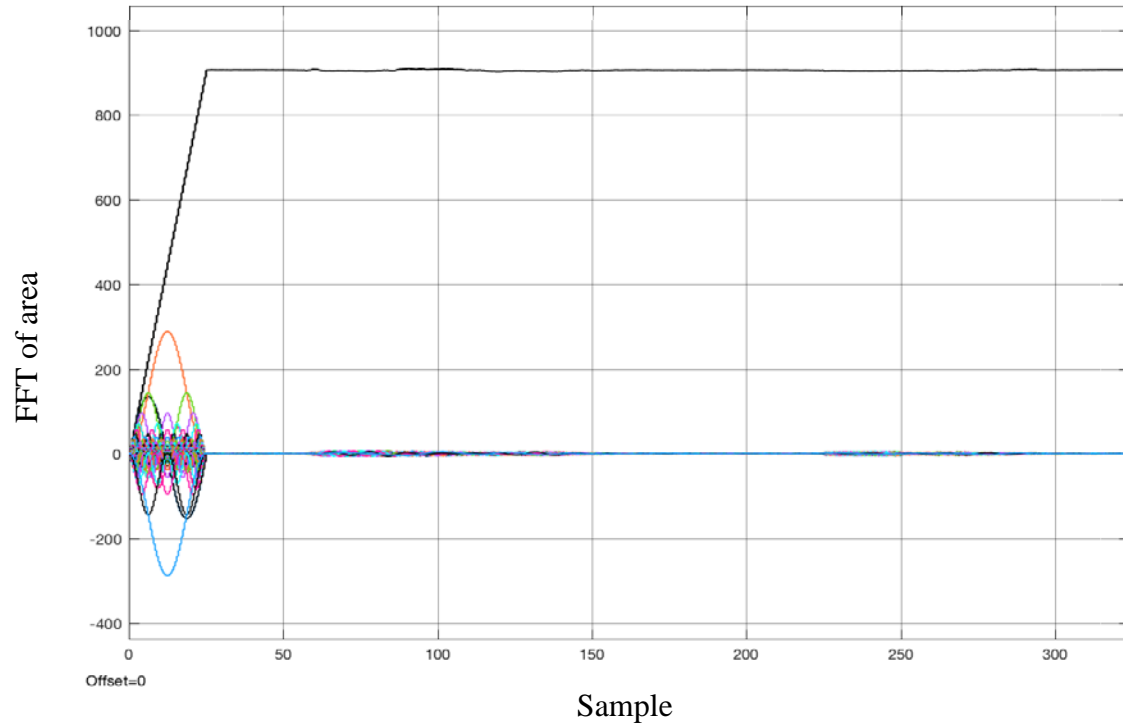


Figure 5.3: Output graph of FFT classification on area

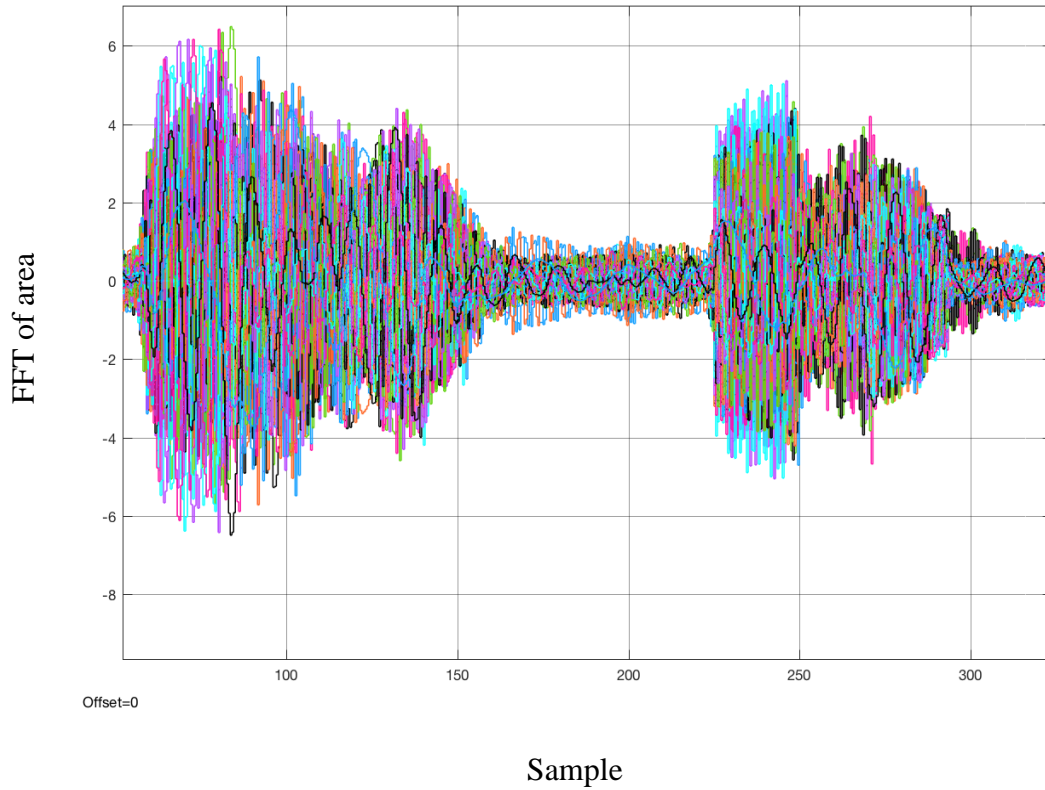


Figure 5.4: Output graph of FFT classification on area (closer view)

Figure 5.4 shows a closer view of the output graph of the FFT classification on the area. It shows all the frequencies of the areas. To get a sample based frequency analysis on area, Figure 5.5 and Figure 5.6 are used. For a better understanding two random samples of frequency (sample 48 and sample 26) are chosen. Figure 5.5 (highlighted) shows frequency at sample 48. Figure 5.6 shows frequency at sample 26.

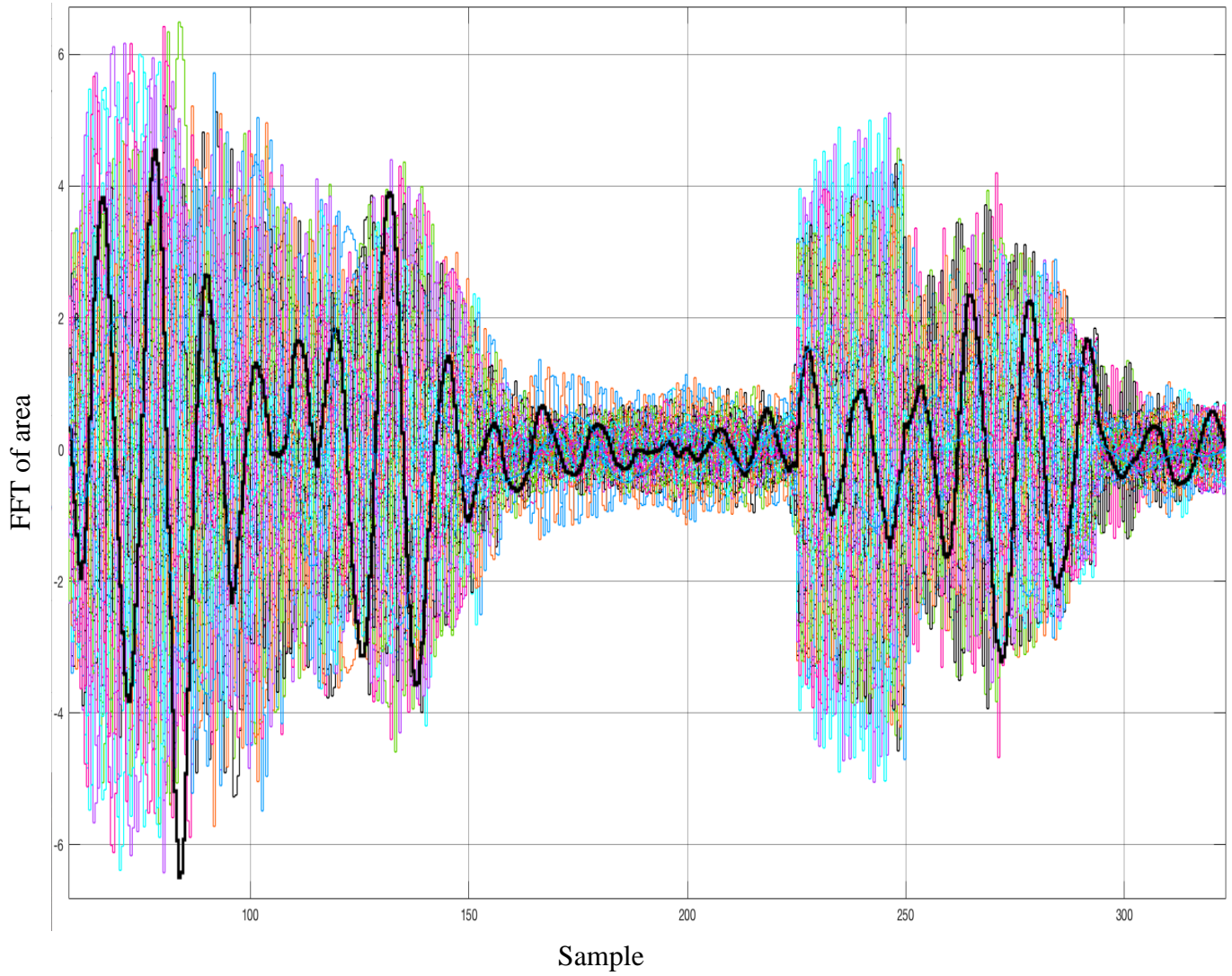


Figure 5.5: Output graph of FFT classification on area (sample 48)

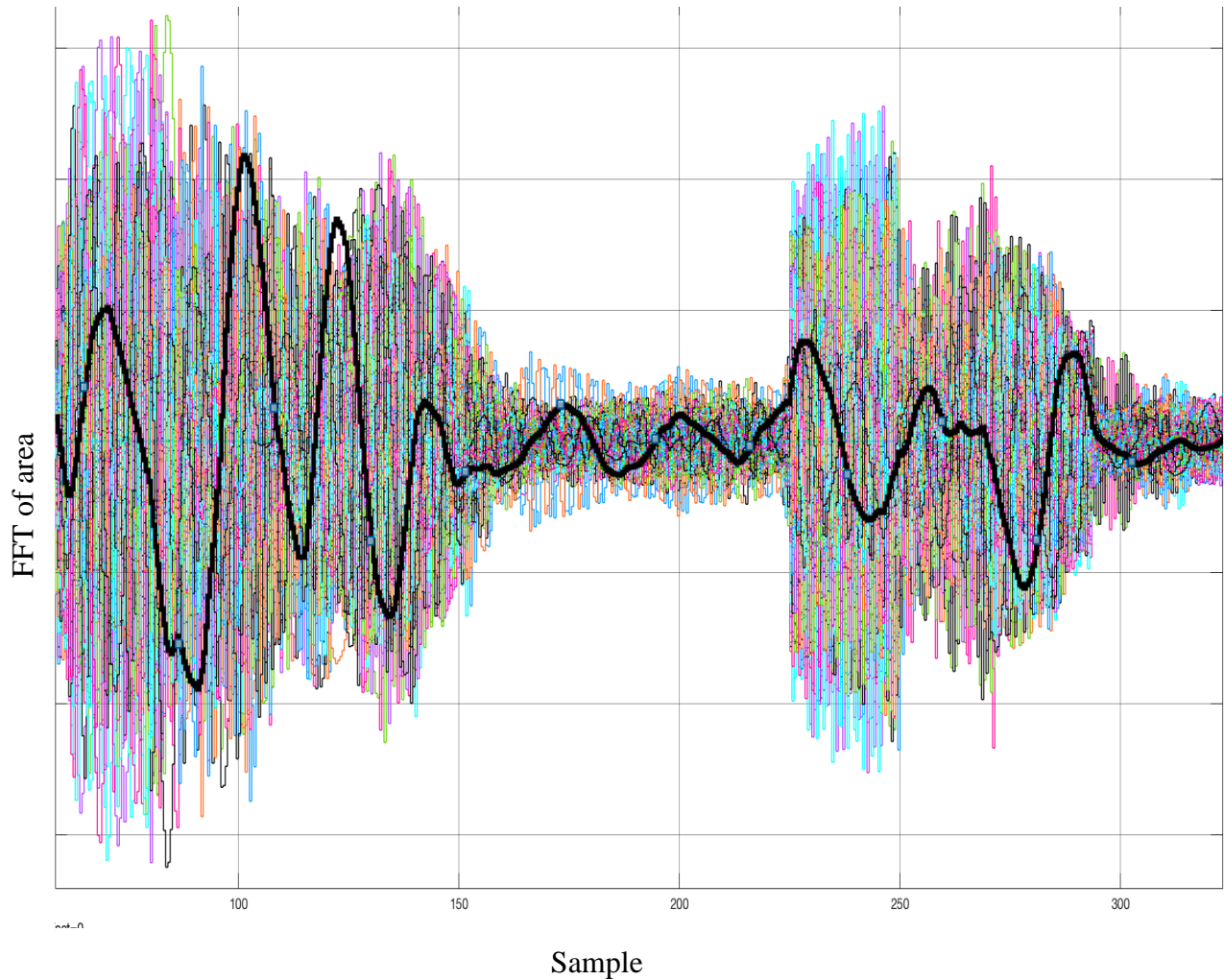


Figure 5.6: Output graph of FFT classification on area (sample 26)

Another feature of the area is studied in order to develop a fuzzy logic controller. In this approach, the angles of the pentagon are studied in order to find useful information for developing a fuzzy inference system. The pentagon has five radii along with the axes of a circle. Figure 5.7 shows a schematic diagram of the pentagon. All five radii are equally distributed. It means the angle between r_1 and r_2 is 72° . This shape has ten internal angles and they are from θ_{12} to θ_{15} .

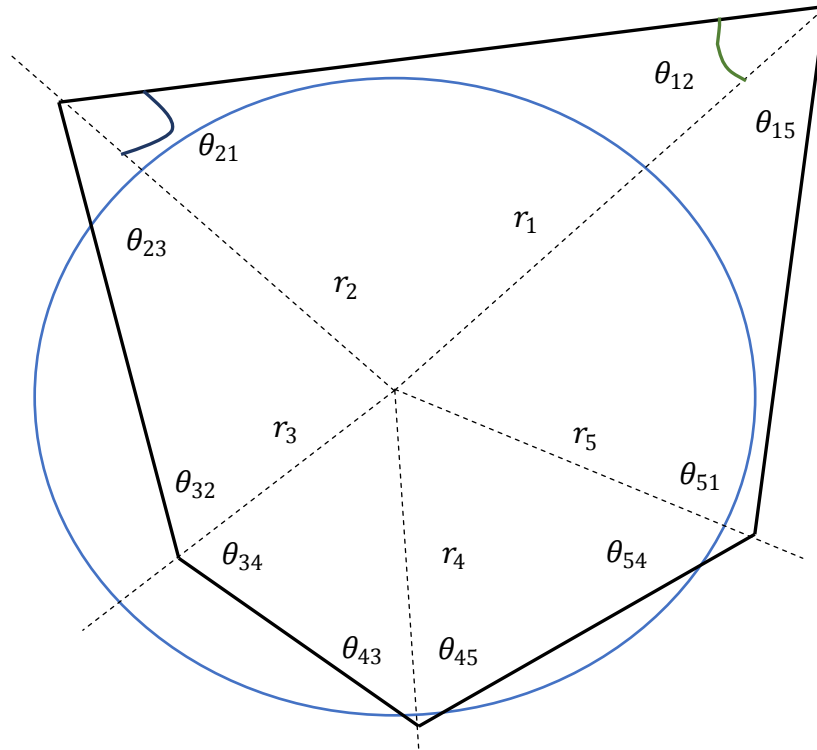


Figure 5.7: Schematic diagram of a pentagon

These ten angles are changing with respect to any forearm movements as the radii are corresponding to the sEMG magnitude recorded. To acquire these ten angles, a *SimulinkTM* program is created [Appendix]. In this *SimulinkTM* program, the angles corresponding to the sEMG signals are processed using a demux block [Appendix]. This demux block helps to see the ten angles separately in a scope block. Figure 5.8 shows the raw data of the ten internal angles during the forearm movements. The first internal angle θ_{12} is considered as Figure 5.8 (a), the second internal angle θ_{21} is considered as Figure 5.8 (b) in column in Figure 5.8, and so on. Two adjacent angles form a pair and are depicted in figure 5.8 in columns opposite to each other. For example, θ_{12} and θ_{21} corresponding to Figure 5.8 (a) and 5.8 (b).

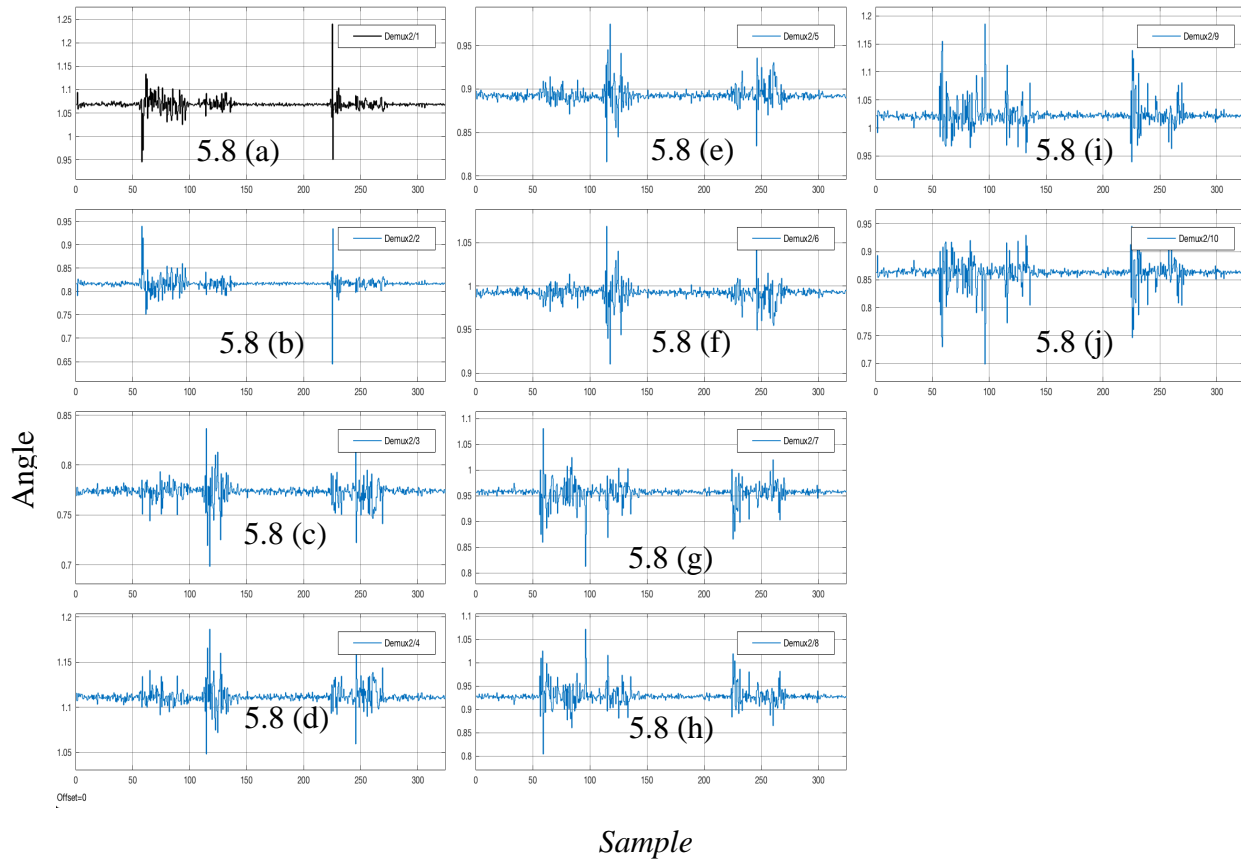


Figure 5.8: Ten internal angles from θ_{12} to θ_{15} (columns first)

Considering angle θ_{12} and θ_{21} , one can observe that when one angle increases, the other decreases. This is true for each pair, i.e. Figures 5.8 (a) and (b); (c) and (d); (e) and (f); (g) and (h); (i) and (j); These ten angles signals are directly correlated with the forearm movements. Another feature method is applied to angle data using the mean value computation as introduced in chapter 2. The means of ten internal angles of the pentagon are plotted in Figure 5.9.

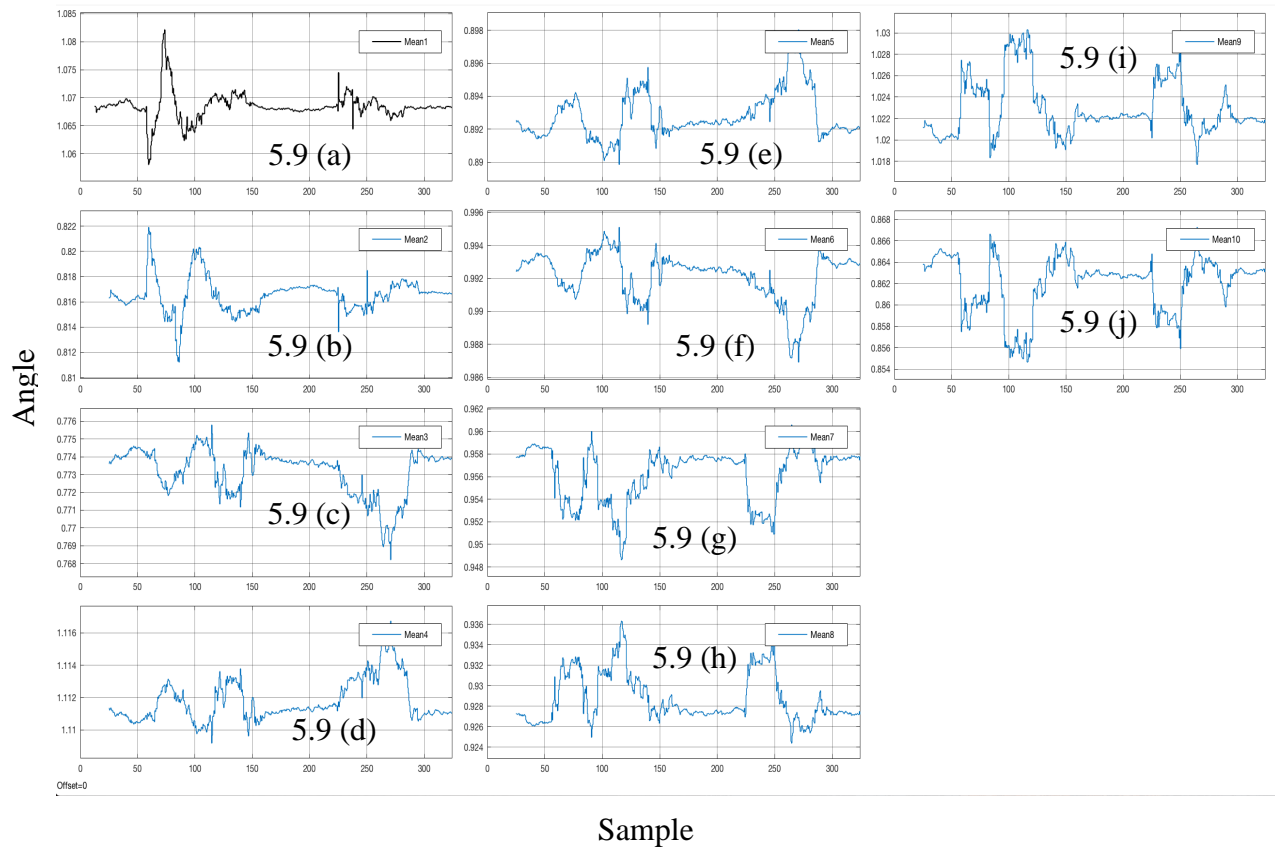


Figure 5.9: Mean of each frame (50 samples slide) for angles from θ_{12} to θ_{15} (columns first)

The first internal angle θ_{12} is considered as Figure 5.9 a), the second internal angle θ_{21} is considered as Figure 5.9 b) in column in Figure 5.9, and so on, similar to Figure 5.8. Figure 5.10 shows the mean of θ_{12} and θ_{21} for a closer view.

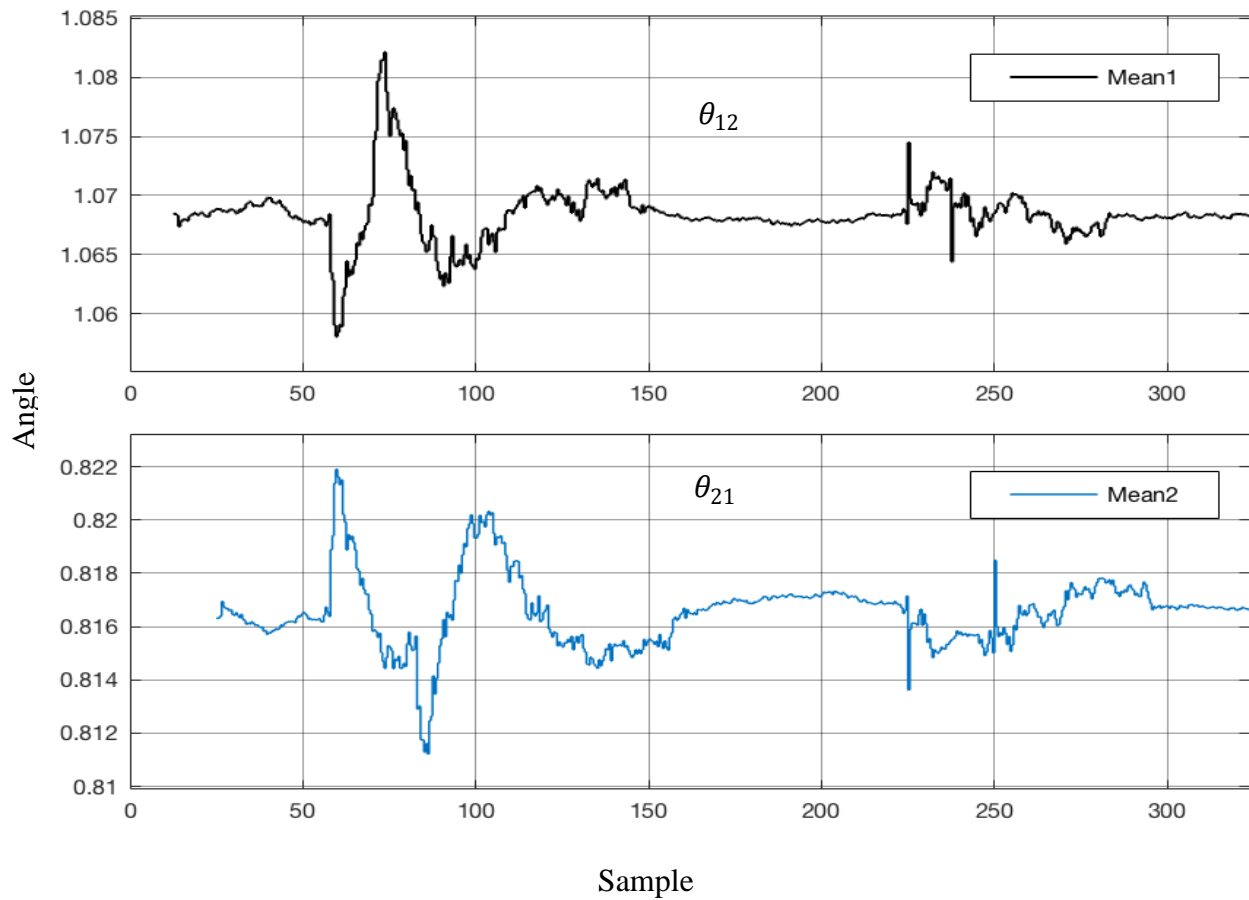


Figure 5.10: Mean of angle θ_{12} and θ_{21}

As described before, two adjacent angles form a pair and they are 180° out of phase. For this reason, five angles are taken for further study instead of ten angles. The selected five angles are $\theta_{12}, \theta_{23}, \theta_{34}, \theta_{45}$ and θ_{51} . The STD classification is done on the angles. The STD classification, as introduced in Chapter 2, is applied on five angles $\theta_{12}, \theta_{23}, \theta_{34}, \theta_{45}$, and θ_{51} . Figure 5.11 shows a graph of the STD classification on the five selected angles.

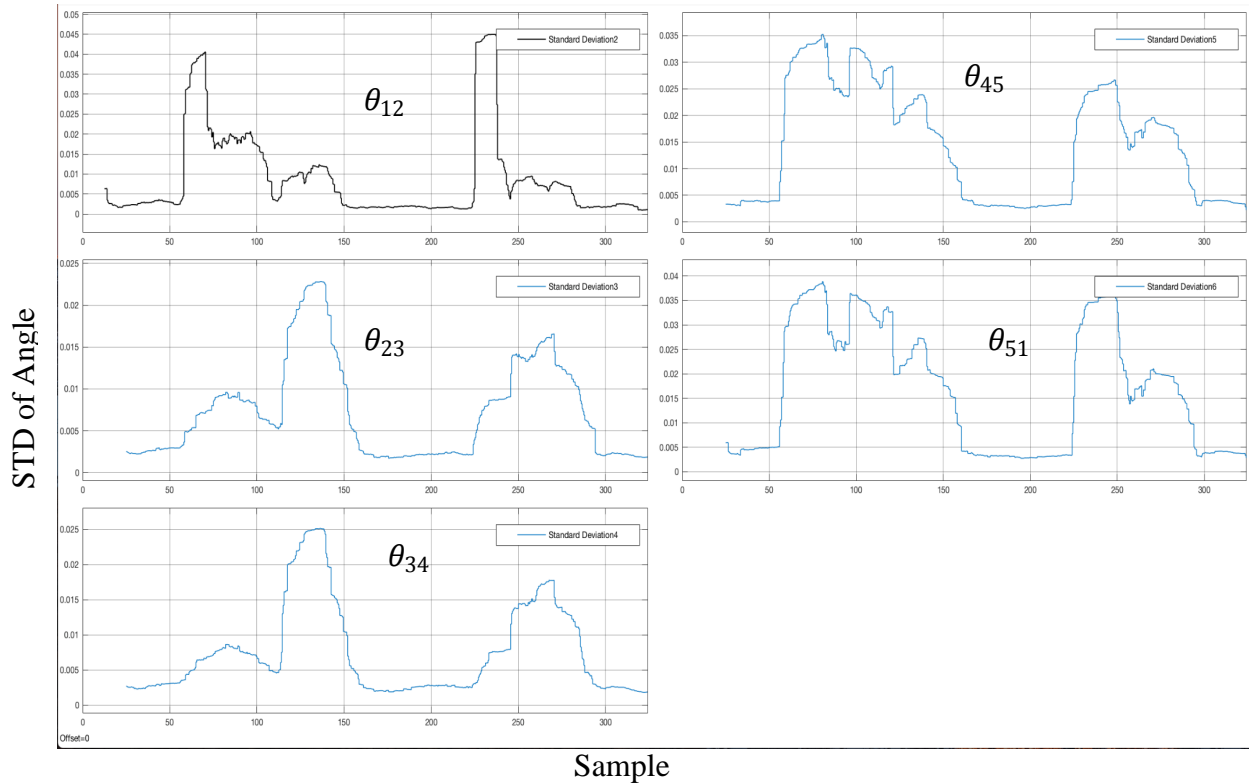


Figure 5.11: STD classification of five angles θ_{12} , θ_{23} , θ_{34} , θ_{45} and θ_{51} (columns first)

STD classification is applied on five angles individually. The effect of the STD classification on each angle is different from another angle. For an inner forearm muscle movement, one angle reacts more than the other angle. The same characteristic is true for the outer forearm muscle movement. Figure 5.12 shows the different responses of angles θ_{12} , θ_{23} , and θ_{34} during the forearm muscle movements.

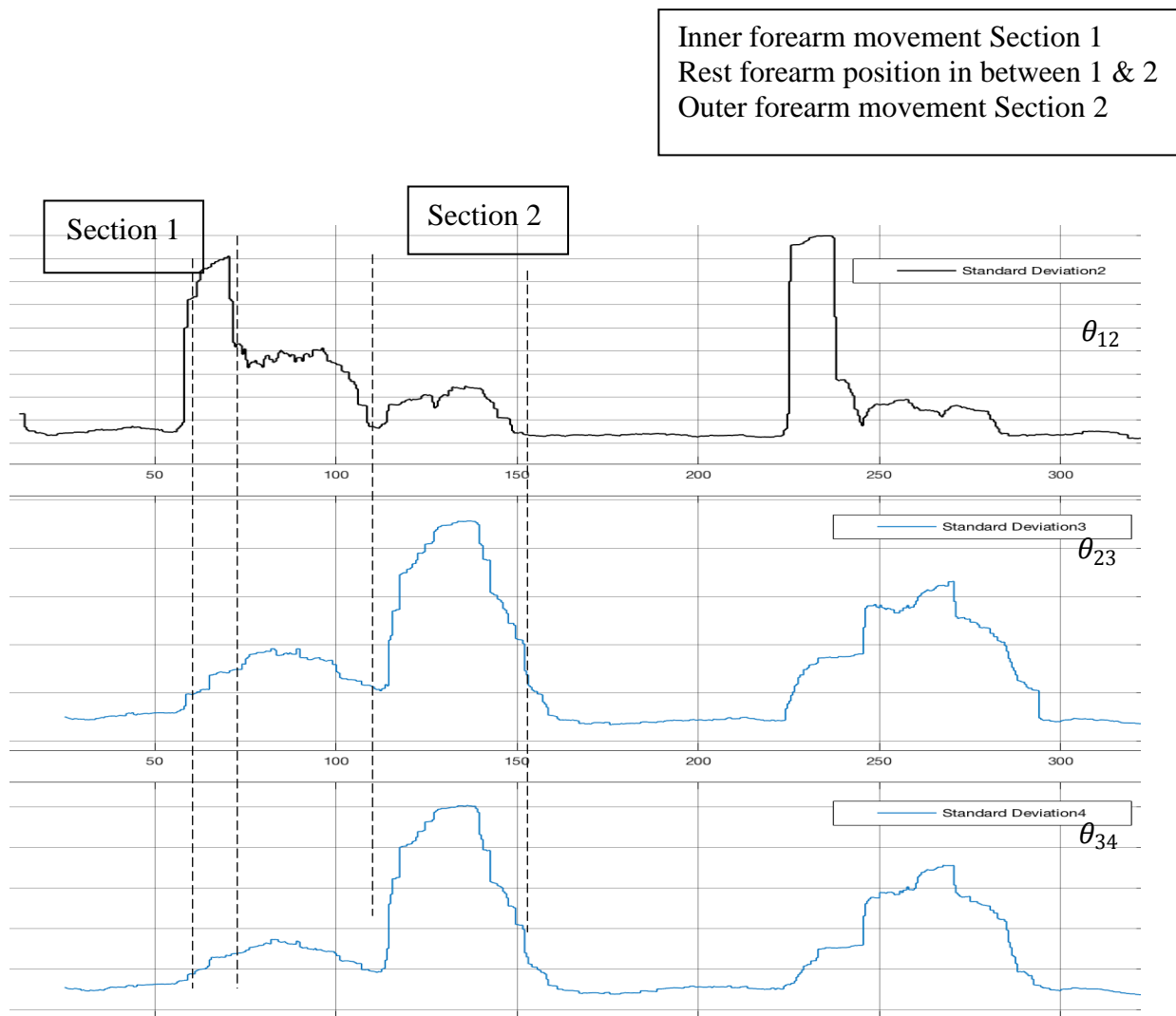


Figure 5.12: STD classification of angles θ_{12} , θ_{23} and θ_{34} (columns first)

For an inner forearm muscle movement, angle θ_{12} reacts more than the angle θ_{34} (Figure 5.12, section 1). On the other hand, angle θ_{12} reacts less than the angle θ_{34} (Figure 5.12, section 2) during the outer forearm muscle movement. The angles θ_{12} and θ_{34} react distinctly. Other angles show less distinct behaviors comparing to θ_{12} and θ_{34} . This distinct behavior can be used for developing a fuzzy inference system. The distinct behaviors of angles θ_{12} and θ_{34} give an indication of which motion is given. By using the feature of the angles θ_{12} and θ_{34} , the inner and

outer forearm muscle movements can be identified by a fuzzy inference system. The data of STD classification of selected angles (θ_{12} and θ_{34}) are used to build a fuzzy logic controller. Chapter 4 describes the steps of the fuzzy logic controller.

5.3 Identification of Motions and Result

The fuzzy logic controller toolbox is used to implement the fuzzy logics as described in Chapter 4 for the purpose of identifying human hand motions. The outer forearm and inner forearm movements are the objective of the identification. These two movements have three stages: inner position, rest position, and outer position as described in Chapter 4. Figure 5.13 shows the output of the fuzzy inference system.

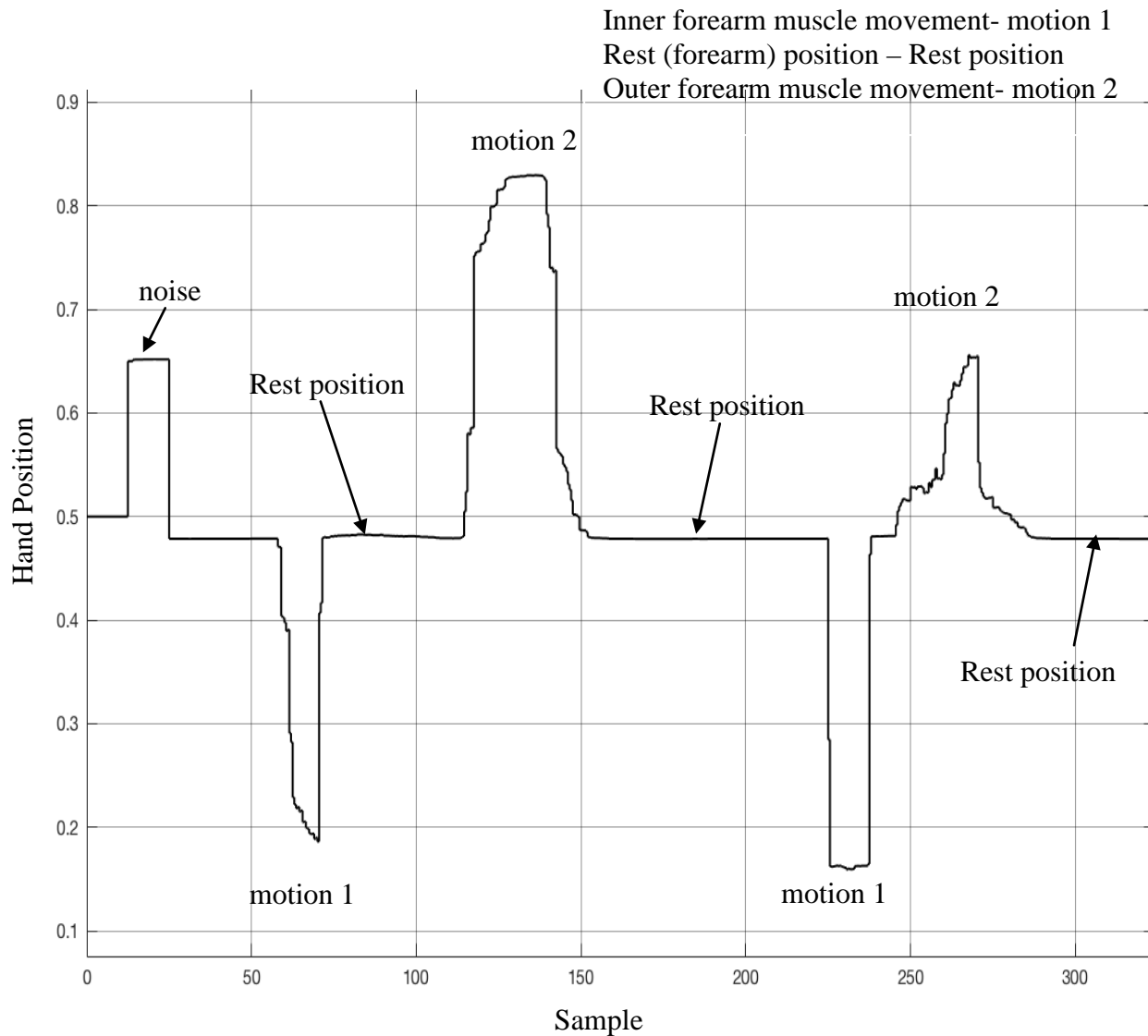


Figure 5.13: Motion identification using fuzzy logic controller

The first peak represents the noise incorporated from the initiation of the experiment. The peak next to the noise (down peak) represents the inner forearm muscle movement. The inner forearm muscle movement is ranged from the samples approximately from 60 seconds to 70 seconds (Figure 5.13, motion 1). The output graph of the STD classification method on the captured area (Figure 5.13) shows the same range. The horizontal line in Figure 5.13 represents the rest position of the forearm meaning no movement is done. The motion 2 in Figure 5.13 represents the outer forearm muscle movement. The range of motion 2 is approximately sample from 121

seconds to 155 seconds. The range of samples of the outer forearm muscle movement is also similar to the output graph of the STD classification method on the captured area (Figure 5.13). Again, the same set of the forearm movements (inner, rest, and outer) are given. Figure 5.14 shows that the fuzzy inference system predicts those movements well. A hysteresis process described in the Appendix is used on the output of the fuzzy logic controller to obtain Figure 5.15. A *Simulink*TM block (relay) is used for this purpose (Appendix).

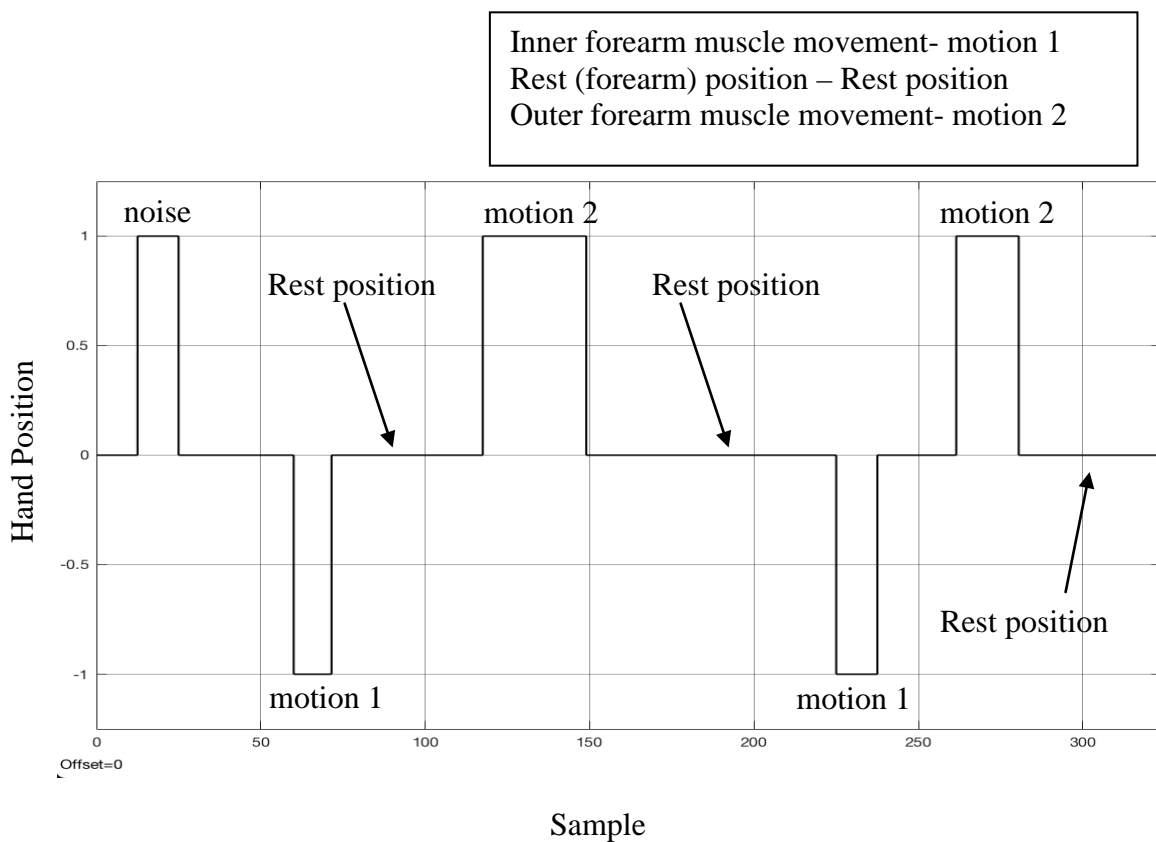


Figure 5.14: Motion identification using fuzzy logic controller(crisp value)

To calculate the error of the prediction, both the actual and targeted outputs are required. Figure 5.15 shows the phase difference of the actual and targeted output. The targeted output is produced from the inner and outer forearm muscle movements as described in the Appendix. The

actual output is also produced with the same movements. The *Simulink*TM model for the actual output is described in the Appendix.

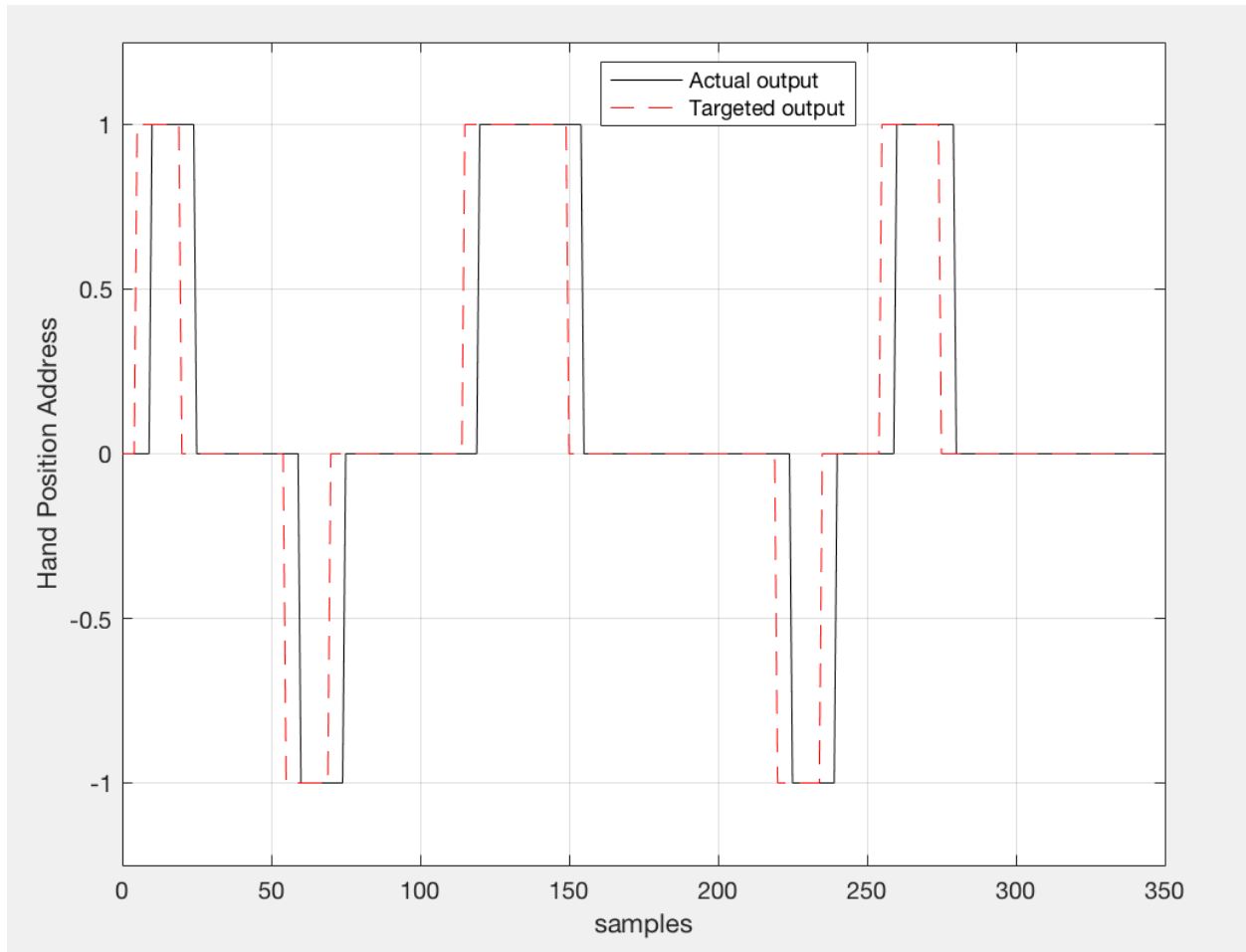


Figure 5.15: Phase difference between actual and targeted output

The red graph represents the targeted output and the solid black graph represents the actual output. There is a phase difference between them. To find the phase difference, correlation coefficient described in Chapter 2 is used. Correction coefficient is a statistical tool which is used to calculate the correlation of two signals. Correction coefficient gives a matrix in *Matlab*TM[Appendix]. The value of the norm of that matrix represents the similarity of the two signals. The norm of the correction coefficient matrix of two identical signals is 2. This value is

used as a reference to calculate the error between actual and targeted output. The norm of the correction coefficient matrix of the actual and targeted output is 1.7380 [Appendix]. This value is compared with standard norm value 2 and it gives 86.9012% similarity between actual and targeted output.

The work is designed based on five sensors, however sensor no. 04 is currently not working due to some technical issues. The sensor can be fixed in the future. Though only four sensors are used in this work, the geometric relation is preserved for the pentagon. The position of sensor no. 04 is considered as a fixed position on the geometric circle.

The developed fuzzy inference system is subjective. It means the motion prediction depends on the electrodes' position on the forearm and the physical condition of the test subject. For a different subject, this fuzzy logic controller is required to be modified with respect to the STD values of the pentagon angles. In the future, more work needs to be done on the captured area of the pentagon using the frequency domain. The FFT data seems to contain additional information that could be used for improving the classification and control results, however, at this time, this is left for future work. The classified sEMG signals can be fed to a Neural Network (NN) for further training purposes.

References

- [1] “Estimating the prevalence of limb loss in the United States: 2005 to 2050” by K. Ziegler-Graham, E.J. MacKenzie, P.L. Ephraim, T.G. Trivison, R. Brookmeyer, Arch Phys Med Rehabil. 2008 Mar;89(3):422-9. doi: 10.1016/j.apmr.2007.11.005.
- [2] “Adaptive control for a five-fingered prosthetic hand with unknown mass and inertia” by Cheng-Hung Chen, Desineni Subbaram Naidu, Marco P. Schoen, WSEAS Transactions on Systems- 10(5):148-161 · May 2011
- [3] “A Heuristic Fuzzy Logic Approach to EMG Pattern Recognition for Multifunctional Prosthesis Control” by Abidemi Bolu Ajiboye and Richard F. ff. Weir, IEEE TRANSACTIONS ON NEURAL SYSTEMS AND REHABILITATION ENGINEERING, VOL. 13, NO. 3, SEPTEMBER 2005
- [4] “sEMG Based Fuzzy Control Strategy with ANFIS Path Planning For Prosthetic Hand” by Chandrasekhar Potluri, Parmod Kumar, Madhavi Anugolu, Steve Chiu, Alex Urfer, Marco P. Schoen, Member, IEEE and D. Subbaram Naidu, Fellow, IEEE, Proceedings of the 2010 3rd IEEE RAS & EMBS International Conference on Biomedical Robotics and Biomechatronics,
- [5] Cram’s “Introduction to Surface Electromyography”, Jones and Bartlett Publishers, ISBN-13: 978-0-7637-3274-5 (pbk.)
- [6] “Neuro-Fuzzy Surface EMG Pattern Recognition For Multifunctional Hand Prosthesis Control” M.Khezri, M. Jahed, Electrical engineering Department- Sharif University of Technology.
- [7] Netter Anatomy Illustration Collection, © Elsevier, Inc.

[8]Peter Konrad, The ABC of EMG: A Practical Introduction to Kinesiological Electromyography, Noraxon INC. USA, Version 1.0 April 2005.

[9]Fridlund AJ, Cacioppo JT. Guidelines for human electro- myographic research. Psychophysiol. 1986;23:567–598.

[10] https://en.wikipedia.org/wiki/Fuzzy_logic.

[11] MS thesis by Pavan Kumar Yarlalagadda, " Real – time sEMG-based finger joint anglecontrol for a smart prosthetic hand," ISU, May 2013.

[12] https://en.wikipedia.org/wiki/Chebyshev_filter

[13] MS thesis by Asib Mahmud “DEVELOPMENT OF A REAL – TIME, ARTIFICIAL NEURAL NETWORK BASED SEMG CLASSIFICATION ALGORITHM FOR MOTION IDENTIFICATION”, ISU, May 2018

[14] MS thesis by Randy C. Hoover “FUSION OF HARD AND SOFT COMPUTING FOR GUIDANCE, NAVIGATION, AND CONTROL OF UNINHABITED AERIAL VEHICLES”, ISU, DECEMBER, 2004.

Appendix

MatlabTM Codes:

01. 1st step to make polar plot of 5 channels equally distributed (360 degree /5)

```
% Polar plot of 5 channels equally distributed.

theta = [0:2*pi/5:2*pi];
theta = theta';
r = [12 13 15 13 12 12]'; % Arbitrary values to plot

figure;
polar(theta, r);
```

02. Overlapping two sets of arbitrary values to see the result

```
r1 = [5 13 13 16 6 5]' % Arbitrary values of radius

r = [r r1];
figure;
polar(theta, r(:,1), 'r');
hold on
polar(theta, r(:,2), 'g');
```

03. For Cartesian Plot:

```
x = r(:,1).*cos(theta);
y = r(:,1).*sin(theta);
figure;
plot(x,y);
```

04. Overlapping two sets of arbitrary values to see the result

```
x1 = r(:,2).*cos(theta);
y1 = r(:,2).*sin(theta);

x = [x,x1];
y = [y,y1];
plot(x(:,1), y(:,1));
hold on;
plot(x(:,2), y(:,2));
```

05. To find the area:

```
a = polyarea(x(:,1), y(:,1));  
a1 = polyarea(x(:,2), y(:,2));
```

06. Simulink for arbitrary sine waves(05) to get visualization of shape changing in real time

```
Function[A, r, theta] = fcn(u1, u2, u3, u4, u5)  
  
N = 5;  
u = [u1, u2, u3, u4, u5]';  
r = [u;u(1,1)];  
theta = [0:2*pi/N:2*pi]';  
  
polar(theta, r, '-o');  
% hold on  
% Convert to cartesian  
x = r.*cos(theta);  
y = r.*sin(theta);  
  
A = polyarea(x,y);  
  
% This is after simulink storing workspace data  
clc;  
% close all;  
n = length(tout);  
  
for i = 1:n  
    polar((theta.signals.values(i,:)),(r.signals.values(i,:)), 'r-  
o');  
    title(i);  
    F(i) = getframe;  
end  
  
movie(F, 1, 9) % 9 frames per sec.
```

07. Code for internal 10 angels

```
function[A, r, theta, theta_ij] = fcn(u1, u2, u3, u4, u5)
%coder.extrinsic('polar');
%coder.extrinsic('theta');

%x=0;
%y=0;

N = 5;
u = [u1, u2, u3, u4, u5]';
%u = [u1, 4, 4, 4, 4]';
r = [u;u(1,1)];
theta = (0:(2*pi)/N:(2*pi))';
polar(theta, r, '-o')
% hold on
% Convert to cartesian
%x = r.*cos(theta);
%y = r.*sin(theta);

[x,y] = pol2cart(theta, r);
A = polyarea(x,y);

theta_ij = [angels(u1, u2); angels(u2, u3); angels(u3, u4);
angels(u4, u5); angels(u5, u1)];

end

function[theta] = angels(r1, r2)

a = sqrt((r2^2) + (r1^2) - 2*r1*r2*cos(72*pi/180));

theta_12 = asin(r2*sin(72*pi/180)/a);
theta_21 = asin(r1*sin(72*pi/180)/a);

theta = [theta_12; theta_21];
end
```

08. Code for error calculation

```
clc;clear all; close all;

load x.mat
load y.mat
% x actual output
% y targeted output
```

```

t = [0:1:349];
plot(t,x,'k', t,y,'--r')
axis([0,350,-1.25,1.25])
grid on;
xlabel('samples');
ylabel('Hand Position Address')
grid on;

legend('Actual output', 'Targeted output')

```

09. Simulink™ modal containing all components

